Space Sci Rev (2009) 145: 193–229
DOI 10.1007/s11214-008-9480-7

# Recent Progress in Physics-Based Models of the Plasmasphere

**Viviane Pierrard · Jerry Goldstein · Nicolas André · Vania K. Jordanova · Galina A. Kotova · Joseph F. Lemaire · Mike W. Liemohn · Hiroshi Matsui**

Received: 9 July 2008 / Accepted: 5 December 2008 / Published online: 23 January 2009


V. Pierrard (✉) · J.F. Lemaire
Belgian Institute for Space Aeronomy (IASB-BIRA), 3 Avenue Circulaire, 1180 Brussels, Belgium
e-mail: viviane.pierrard@oma.be

J.F. Lemaire
e-mail: lemaire@astr.ucl.ac.be

V. Pierrard · J.F. Lemaire
Center for Space Radiations (CSR), Louvain-La-Neuve, Belgium

J. Goldstein
Space Science and Engineering Division, Southwest Research Institute (SwRI), San Antonio, TX, USA
e-mail: jgoldstein@swri.edu

N. André
Research and Scientific Support Department (RSSD), ESTEC/ESA, Noordwijk, The Netherlands
e-mail: nandre@rssd.esa.int

V.K. Jordanova
Space Science and Applications, Los Alamos National Laboratory (LANL), Los Alamos, NM, USA
e-mail: vania@lanl.gov

G.A. Kotova
Space Research Institute (RSSI), Russian Academy of Science, Moscow, Russia
e-mail: kotova@iki.rssi.ru

M.W. Liemohn
Atmospheric, Oceanic, and Space Sciences Department, University of Michigan, Ann Arbor, MI, USA
e-mail: liemohn@umich.edu

H. Matsui
University of New Hampshire (UNH), Space Science Center Morse Hall, Durham, NH, USA
e-mail: hiroshi.matsui@unh.edu

**Abstract** We describe recent progress in physics-based models of the plasmasphere using the fluid and the kinetic approaches. Global modeling of the dynamics and influence of the plasmasphere is presented. Results from global plasmasphere simulations are used to understand and quantify (i) the electric potential pattern and evolution during geomagnetic storms, and (ii) the influence of the plasmasphere on the excitation of electromagnetic ion cyclotron (EMIC) waves and precipitation of energetic ions in the inner magnetosphere. The interactions of the plasmasphere with the ionosphere and the other regions of the magnetosphere are pointed out. We show the results of simulations for the formation of the plasmapause and discuss the influence of plasmaspheric wind and of ultra low frequency (ULF) waves for transport of plasmaspheric material. Theoretical models used to describe the electric field and plasma distribution in the plasmasphere are presented. Model predictions are compared to recent CLUSTER and IMAGE observations, but also to results of earlier models and satellite observations.

**Keywords** Plasmasphere · Models · Fluid · Kinetic · CLUSTER · IMAGE

## 1 Introduction

The satellites IMAGE (Imager for Magnetopause to Aurora Global Exploration) and CLUSTER have notably provided global views of the plasmasphere and electron density profiles that are especially useful in the study of plasmapause formation (De Keyser et al. 2008, this issue). Since the limit of the plasmasphere was discovered (Gringauz et al. 1960) and named plasmapause by Carpenter (1966), different mechanisms have been suggested to explain this sharp boundary, as recalled in Pierrard and Stegen (2008). Dynamical simulations of the plasmasphere have been developed beginning with simple simulations in a spatially constant electric field (Grebowsky 1970) and have since become more sophisticated.

Recent progress in plasmasphere and plasmapause simulations is described using the fluid and the kinetic approaches. This paper is divided in three main sections: The first describes the recent improvements in fluid models related to CLUSTER and IMAGE observations, the second describes such improvements in kinetic models, and the third compares the two approaches and show recent developments based on other satellite observations. Such models concern also the density distributions along the magnetic field lines and refilling processes.

In the fluid section, Sect. 2.1 describes the influence of the inner magnetospheric electric potential on the plasmasphere. The couplings of the plasmasphere with the ionosphere and the magnetosphere play important roles that are described in Sects. 2.2 and 2.3.

In the kinetic section, the mechanisms of plasmapause formation are described in Sect. 3.1. The postulated existence of the plasmaspheric wind and its implications are discussed in Sect. 3.2. The global transport of plasmaspheric material by ULF waves is presented in Sect. 3.3. Models of electrostatic potential and field aligned distribution of the plasma in an ion-exosphere are respectively described in Sects. 3.4 and 3.5. The refilling processes are studied in Sect. 3.6, as well as the Coulomb collisions and implications of Monte Carlo simulations.

Finally, Sect. 4 discusses the comparison between the kinetic and magnetohydrodynamic (MHD) approaches for time-dependent models.

The empirical plasmasphere models directly based on satellite observations are presented elsewhere in this issue (Reinisch et al. 2008). In the present paper, we focus mainly on the physical processes implicated in the plasmaspheric models. The basic plasmaspheric

theoretical concepts and ideas that flourished during the past forty years have been discussed in research articles and review papers that are listed by Lemaire and Gringauz (1998) and in more recent reviews like that by Kotova (2007). Some theoretical concepts are recalled but we mainly emphasize in the present paper the progress obtained from the IMAGE and CLUSTER missions.

## 2 The Fluid Approach

### 2.1 Inner Magnetospheric Electric Potential

Progress has been made recently in using plasmaspheric simulations (as well as simulations of the ring current and its coupling to the ionosphere) to understand and quantify the electric potential pattern and evolution during magnetic storms. This progress has been achieved via a series of simulation studies, ranging from simple test particle simulations to full fluid simulations, employing a variety of electric potentials, both parametric and self-consistent. Comparison of simulation results with global images obtained by the IMAGE spacecraft (Burch 2000) has played a key role alongside in-situ observations.

Decades of simulation work, beginning with simple test particle simulations in a spatially constant electric field (Grebowsky 1970; Chen and Wolf 1972; Chen et al. 1975) and followed by numerous more sophisticated fluid treatments (Spiro et al. 1981; Elphic et al. 1996; Lambour et al. 1997; Weiss et al. 1997) all predicted that plasmaspheric plumes form and evolve in response to enhanced convection. Plumes are described in detail elsewhere in this issue (Darrouzet et al. 2008). Nonetheless, the predictions of models such as these were not universally accepted (e.g., Chappell 1972; Lemaire and Gringauz 1998), and the existence of plumes was not conclusively proven until the advent of global images by the IMAGE Extreme UltraViolet (EUV) imager (Sandel et al. 2000) that clearly showed global plume development in so-called "phases" in accord with the early models (Goldstein et al. 2003c; Spasojević et al. 2003; Goldstein and Sandel 2005). However, though the plumes recorded by EUV images did follow the predicted phases in a global sense, on a sub-global scale numerous storm-time behaviors and density features remained unexplained such as plasmapause "crenulations" (Spasojević et al. 2003) and azimuthally-localized "notches" spanning several $L$-shells (Gallagher et al. 2005). Most studies of these (and many other) density features concluded that knowledge of the inner magnetospheric electric field, (especially on sub-global scale sizes) remains inadequate, though a parallel line of investigation suggested that plume formation is primarily driven by forces other than convection that in principle can explain some of the novel density features (Lemaire 2000).

Inner magnetospheric shielding (Jaggi and Wolf 1973) was proposed long ago as a mechanism whereby the influence of solar-wind-driven convection would be lessened earthward of the region 2 current system linking the ring current to the ionosphere; however, for decades the influence of shielding was difficult to quantify. Using fluid simulations with an empirical inner magnetospheric potential whose parameterization was based on earlier self-consistent results of the Rice Convection Model (RCM), shielding was shown to have a palpable effect on the recovery-phase plasmapause structure, producing shoulder-shaped bulges 0.5 Earth radius ($R_E$) or larger (Goldstein et al. 2002, 2003d). That these models agreed with EUV images was taken as proof of at least partial shielding of the inner magnetosphere, but self-consistent RCM runs also illustrated the almost complete breakdown of shielding during the strongest storms (Sazykin et al. 2005).

On the other hand, ring-current-ionosphere coupling via region 2 currents can also intensify the radial electric field especially in the dusk-to-midnight local time (LT) sector, producing a radially-narrow, azimuthally-directed flow channel (Galperin et al. 1974; Smiddy et al. 1977; Burke et al. 1998; Anderson et al. 2001) that in recent years has come to be known as the sub-auroral polarization stream (SAPS) (Foster and Burke 2002). Used in test particle simulations, empirical models of SAPS have achieved reasonable success at reproducing the plasmapause and plume locations observed by IMAGE EUV and Los Alamos National Laboratory (LANL) geostationary satellites (Goldstein et al. 2003a, 2005a, 2005b). Nonetheless it is clear that only a self-consistent formulation with realistic ring current pressure distributions, region 2 currents, and ionospheric conductivities can hope to truly capture the dynamical development -both global and local- of SAPS or, for that matter, shielding.

Illustrating this point, Liemohn et al. (2004, 2005, 2006) conducted a series of studies comparing plasmaspheric simulation results against observations, using a variety of electric field descriptions and calculational formulations, in order to decipher the true electric field dynamics during the storm events. The plasmaspheric model used in these studies is the Dynamic Global Core Plasma Model (DGCPM) of Ober et al. (1997). This code solves a continuity equation for the flux tube content of cold "thermal" ions, using second-order accurate numerical schemes to convect the ions from one grid cell to another. The code is flexible and modular, capable of using any magnetic or electric field specification and written in subroutine format for easy coupling to other codes. For Liemohn et al. (2004, 2005, 2006) studies, the DGCPM was linked with the Ring current Atmosphere interaction Model (RAM) (Jordanova et al. 1996a; Liemohn et al. 2001) along with the ionospheric electric potential solver of Ridley and Liemohn (2002). The two-way coupling between these codes allows for the ring current to alter the inner magnetospheric electric field, which in turn changes the plasmaspheric morphology, which then collisionally interacts with the ring current. Field-aligned currents (FACs) are calculated from the RAM hot plasma distribution, and these are mapped along the magnetic field to 120 km altitude where they are used as current sources and sinks for the ionosphere potential solver. The resulting potential then mapped back to the magnetosphere for use in the next time step of RAM and DGCPM. To obtain a local density at a particular place within the magnetosphere from the total content values calculated by DGCPM, a field-line density distribution must be assumed. This distribution is usually taken to be $n/B =$ constant where $n$ is number density and $B$ is magnetic field strength, although any relationship could be chosen.

Liemohn et al. (2004) examined the electric potential structure and resulting plasmaspheric morphologies for three electric field descriptions: a simple two-cell convection pattern (McIlwain 1986; Liemohn et al. 2001), the Weimer empirical model (Weimer 1996), and a self-consistent potential model (Ridley and Liemohn 2002) driven by field aligned currents closing the partial ring current (as calculated by a simultaneously-running ring current model). The storm on 17 April 2002 was chosen for this investigation because it is a simple "single-dip" event caused by a shock-sheath passage ahead of a magnetic cloud (which caused a subsequent storm on 18 April).

They compared the DGCPM results against plasmapause locations extracted from snapshots from the EUV instrument onboard the IMAGE spacecraft. Figure 1 shows the method of data-model comparison. In the EUV image (Fig. 1a), a sharp intensity decrease can be seen where the thermal plasma density suddenly drops. This is interpreted as the plasmapause and its location is manually recorded. In the DGCPM equatorial density results (Fig. 1b) using a self-consistent electric field, it is often hard to distinctly identify such a boundary, and therefore the density gradient is numerically calculated (Fig. 1c). This quantity clearly shows the sharp drop in plasmaspheric density, and the peak gradient along any

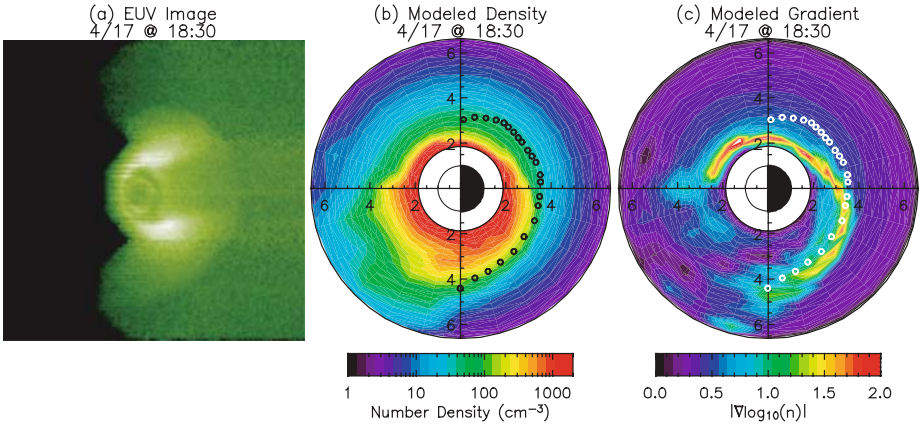


**Fig. 1** Example data-model comparison (at 18:30 UT on 17 April 2002) between an IMAGE EUV snapshot and a DGCPM plasmasphere result. Shown here is **a** an EUV image (count rates per pixel) on a linear green-shade color scale, **b** DGCPM equatorial plane cold plasma densities on a logarithmic color scale, and **c** the magnitude of the gradient of the logarithm of the density from DGCPM on a linear color scale. In the EUV image, the view is over the North Pole with the Sun off to the left and slightly downward, as indicated. In the model results, the view is over the North Pole with the Sun directly to the left, and distances are given in $R_E$. In the image, the plasmapause is the steep drop in intensity from light green to darker green. The extracted plasmapause from this image is shown in the model results as *circles*. (Adapted from Liemohn et al. 2005)

given radial slice is designated the plasmapause. These two radial distances can then be directly compared (as a function of LT and universal time UT).

It was found that the selected two-cell convection model (McIlwain 1986; Liemohn et al. 2001) is good at predicting the nightside plasmapause location, particularly in the post-midnight sector. However, the small electric fields on the dayside from this model yield incorrect dayside morphologies for the stormtime plasmasphere, at least during the recovery phase of the storm. The Weimer electric field model (Weimer 1996) yields a better dayside description of the plasmapause, particularly regarding the shape of the plasmaspheric plume relative to that produced by the modified McIlwain description. The electric fields are somewhat too strong in the inner magnetosphere, though, resulting in a systematically smaller plasmasphere than those extracted from the observations. The self-consistent electric field model yielded the best comparison with the observed plasmaspheric plume location. However, a too low imposed conductance in the post-midnight region led to a modeled plasmapause that was inward of that observed in this magnetic local time (MLT) quadrant.

The second study in the series (Liemohn et al. 2005) was a systematic analysis of the self-consistent electric field choice. In particular, the ionospheric conductance needs to be specified in the model, and the settings for defining this parameter can be altered within reasonable limits. This conductance model has sources from sunlight on the dayside, starlight (applied everywhere), and a smooth auroral oval of high conductance. The first objective of this study was to conduct a parametric examination of the response in the numerical simulation results to various settings for the nightside ionospheric conductance. The second objective was to compare these results against observations to determine whether (and why) these systematic changes in the conductance bring the simulation results closer to reality. Like Liemohn et al. (2004), this study focused on the 17 April 2002 storm event.

There are five ways in which the conductance was changed between the simulations performed for this study. The first was the amplitude of the oval conductance peak, which

varies in time according to the relation used by Ridley et al. (2004). Because those formulas were developed for region 1 current intensities, a scaling factor was included to account for the known offset in magnitude between region 1 and region 2 currents (e.g., Iijima and Potemra 1976; Weimer 1999). Liemohn et al. (2005) found that a higher multiplier setting (i.e., high conductance) resulted in a smaller plasmasphere.

A second parameter varied in the conductance model was the latitudinal location of the oval peak relative to the RAM-generated FAC peak. The oval is a product of both region 1 and region 2 currents, and RAM is only calculated in the latter, so the oval peak should be shifted poleward of the calculated FAC peak. The data-model comparisons revealed an optimal oval shift of five degrees; too much or too little poleward resulted in a less intense electric field across the dusk sector and a poor plume location in the plasmaspheric model results.

A third parameter was the dawn-to-dusk tilt of the auroral oval. It is known that precipitating electrons are the major contributor to this conductance, and their drift paths bring them closer to the Earth on the dawn side than on the dusk side of the inner magnetosphere. It was found that a symmetric oval (with no tilt) best matched the observations, and moving the dawnside oval equatorward made the plasmapause less distinct across that sector.

The fourth parameter was the choice of the potential description applied at the high-latitude boundary of the Poisson equation. Two models are used for this boundary condition: a ring of potential values extracted from the Weimer model and a sine wave description using only the cross polar cap potential difference from the Weimer model. Not surprisingly, it was concluded that the former choice produced the better fit to the observed plasmapause locations.

The final free parameter that was varied is the baseline conductance value, the so-called starlight Pedersen conductance (Strobel et al. 1974). The baseline (that is, non-auroral) ionospheric conductance at any given place on the nightside is not well known, but it is a function of the illumination from stars and scattered sunlight, from the length of time that part of the atmosphere has been in darkness, transport effects, plasmaspheric downflow, and local heating influences. The influence was small, but increasing this background conductance value resulted in a slightly smaller plasmasphere (similar to the first parameter, the peak conductance multiplier).

The third paper in the sequence (Liemohn et al. 2006) was a large data-model comparison study for two storm intervals (22 April 2001, and 21–23 October 2001). The overall goal of this effort was to determine the state of the inner magnetospheric electric field throughout these two storms. The RAM-DGCPM model combination was run with four electric field specifications, and these results were compared with numerous observations of the plasmasphere and ring current to determine which field selection performed best at which times and places. The specific electric field choices were the Volland-Stern two-cell convection pattern (Volland 1973; Stern 1975), the modified McIlwain two-cell model (McIlwain 1986; Liemohn et al. 2001), and two versions of the self-consistent electric field (Liemohn et al. 2004), with two different peak conductance multiplier values.

In addition to the EUV-DGCPM comparisons conducted in the earlier studies, Liemohn et al. (2006) also included comparisons against in-situ plasmaspheric observations. Specifically, densities and velocities were calculated from the low-energy ion population as measured by the Magnetospheric Plasma Analyzer (MPA) instruments onboard the geosynchronous LANL satellites.

At geosynchronous orbit (6.6 $R_E$ geocentric distance), storm-time plasmaspheric observations are limited to the afternoon LT sector, when the satellites cross the plasmaspheric plume. Figure 2 shows a comparison between the plasmaspheric densities recorded by the

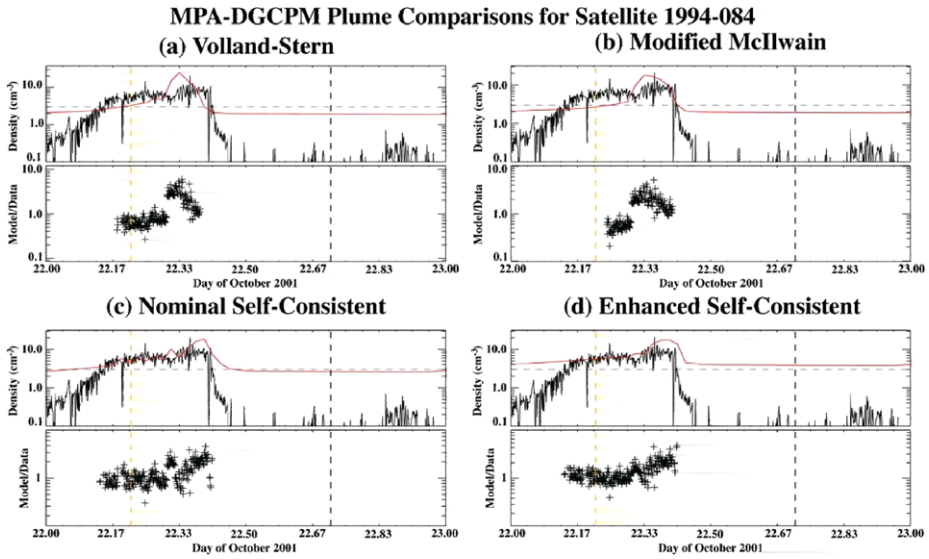


**Fig. 2** Four pairs of plots showing a comparison between the low-energy ion density from the MPA instrument on the geosynchronously-orbiting LANL084 spacecraft to corresponding simulated plasmaspheric density values from the runs with four different field descriptions of Liemohn et al. (2006). In each pair, the *upper panel* (**a** and **b**) shows the density comparison while the *lower panel* (**c** and **d**) shows the ratio of the modeled value to the data value. In the *upper plot*, the data is shown in *black* and the simulation results in *red*. In the ratio plots, values are only shown when both the modeled and the observed density is greater than $3\,\mathrm{cm}^{-3}$. This is an empirically-determined cut-off signifying plasmaspheric plume observations, and therefore trustworthy moment values. This cut-off is marked in the *upper panels* with a *horizontal black dashed line*. The *vertical black* and *yellow dashed lines* indicate local midnight and noon, respectively

LANL 084 satellite with results from the four simulations of DGCPM during the 21–23 October 2001 storm. It is seen that the four numerical results have varying degrees of goodness of fit against the data. In particular, there seems to be two components to the plume, with a slight dip in density at 07:00 UT on 22 October 2001. The self-consistent electric field results produce a similar feature, while the two simplistic two-cell models do not.

Liemohn et al. (2006) found that the self-consistent electric field descriptions did the best at reproducing the data throughout these storm intervals. An interesting result is that the shielded Volland-Stern electric field model, driven with the 3-hour $K_p$ index, also did quite well in the data-model comparisons. In particular, this simple model was excellent at reproducing the main phase plasmapause structure, including the plume location as seen by two different data sets. However, the Volland-Stern model was irregular in its ability to reproduce the observations, often being good against some data sets but off against others.

The two self-consistent field simulations were much more regular with respect to which data sets they obtained excellent agreement, and they matched these data sets throughout the interval (rather than just at certain times and places). The modified McIlwain field consistently produced the worst plasmaspheric data-model comparisons of the 4 field choices, although there were times (particularly the main phase) when it also accurately matched the observed plume characteristics.

### 2.2 Plasmasphere-Ionosphere Coupling

Another aspect of global plasmaspheric dynamics is the essential mass-exchange interaction between the plasmasphere and ionosphere. Outflow from the ionosphere can gradually fill (or refill) plasmaspheric flux tubes with cold plasma, moving the plasmapause location outward over the course of several hours or days; on the other hand, storm-time "dumping" of plasmaspheric material into the ionosphere can deplete flux tubes well inside the plasmapause. Though some fluid simulations have attempted to include ionospheric refilling (Lambour et al. 1997; Weiss et al. 1997; Goldstein et al. 2002), these treatments have been fairly simple empirical constraints on an otherwise decoupled plasmasphere model. However, the availability of global plasmasphere images has encouraged progress in this area as well.

As an example of this progress, in this section the temporal evolution of plasma density in the equatorial plane of the magnetosphere is studied with a two-dimensional model of the plasmasphere developed by Rasmussen et al. (1993). This model includes the supply and loss of hydrogen ions due to ionosphere-magnetosphere coupling as well as the effects of $\boldsymbol{E} \times \boldsymbol{B}$ convection. It utilizes a method for modeling the transport of thermal plasma in the equatorial plane pioneered by Chen and Wolf (1972) that achieves considerable simplification and reduces computer costs. A conservation equation for the total content of a flux tube is obtained by integrating the continuity equation along a flux tube from ionosphere to conjugate ionosphere; the motion of individual flux tubes due to the $\boldsymbol{E} \times \boldsymbol{B}$ drift is then followed. Changes of the total tube content due to fluxes of particles entering (or leaving) the plasmasphere from conjugate ionospheres are described with a parametric model, which utilizes the Mass-Spectrometer-Incoherent-Scatter (MSIS) model (Hedin 1987) of the neutral atmosphere and the International Reference Ionosphere (IRI) model (Bilitza 1986). This method is applicable for some types of plasmaspheric studies, including those considering plasmapause formation and the detachment of plasmaspheric plumes, when complete information along a flux tube is not required. In many instances, the convection electric field causes a more rapid variation in density than does any other process. Time scales for advective changes in density can be of the order of one hour or less. This compares to time scales for refilling which are of the order of a few days or longer.

The evolution of the plasmaspheric electron density during 17–19 June, 2001 obtained with the model of Rasmussen et al. (1993) is shown in Fig. 3. During this period there was a moderate geomagnetic storm with minimum $Dst = -61$ nT and maximum $K_p = 5^+$. The plasmasphere model of Rasmussen et al. (1993) was coupled with the RAM (Jordanova et al. 1996a, 2007) and was driven by a high time resolution convection electric field model and a dipole model of the Earth's magnetic field. For these simulations Jordanova et al. (2007) used the tabulated value of the auroral boundary index (ABI) to control the strength of the convection, by first converting it to an effective $K_p$ (Gussenhoven et al. 1981) and then using a Volland-Stern type electric field with a shielding parameter of 2 (Volland 1973; Maynard and Chen 1975; Stern 1975). During periods of increased convection (larger $K_p$ index) the plasmasphere was eroded on the nightside, and at larger $L$-shells enhanced densities were confined to the postnoon plasmaspheric plumes.

As the activity level decreased, the plasmasphere corotated and expanded, refilling from the ionosphere. The diamond symbols in Fig. 3 indicate the model plasmapause, i.e., the location of a steep gradient in electron density, identified in the model as the region where the density drops by a factor of 5 or more over a radial distance of 0.25 $R_E$. The solid line in Fig. 3 shows the plasmapause identified from IMAGE EUV data as a density drop below the sensitivity threshold of the instrument, estimated to be roughly 40 $\pm$ 10 electrons

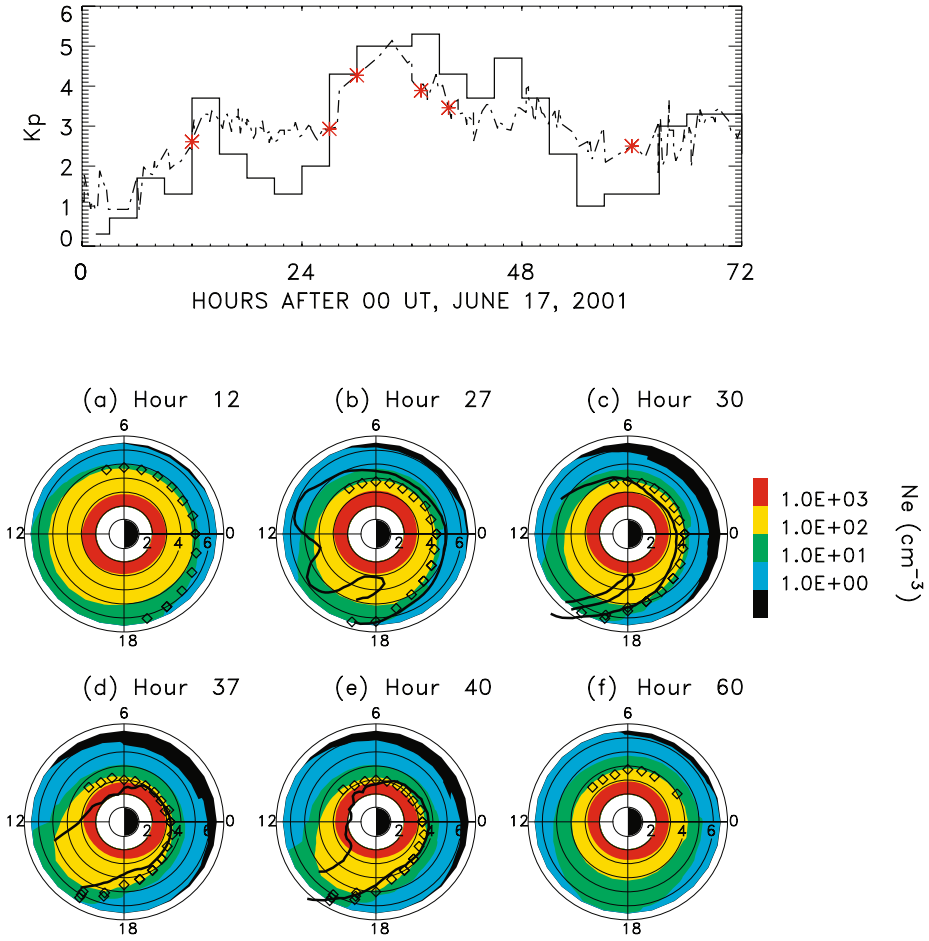


**Fig. 3** (*Top*) The 3-hour index $K_p$ (*solid*) and the effective $K_p$ determined from the auroral boundary index (*dashed-dotted line*). **a–f** Equatorial plasmaspheric electron densities (cm$^{-3}$) at selected hours after 00:00 UT on 17 June 2001 indicated with stars on the $K_p$ plot. The *diamonds* indicate the model plasmapause (Jordanova et al. 2007) while the *solid line* indicates the plasmapause location determined from IMAGE EUV data. (Adapted from Jordanova et al. 2007)

cm$^{-3}$ (Goldstein et al. 2003b). These authors showed that the $He^+$ edge coincides with the plasmapause by comparing the $L$-shell of steep electron density gradients, extracted from passive mode dynamic spectrograms recorded by the IMAGE Radio Plasma Imager (RPI) with the $L$-shell of EUV $He^+$ edges obtained when the satellite is outside the plasmasphere near apogee. The model reproduced well the duskside plasmapause location determined from EUV data on 18 June 2001. However, the model predicted larger densities near 13:00–15:00 MLT than observed by the EUV imager at hour ∼40 (Fig. 3e). Comparing simulations of the 21 October 2001 large geomagnetic storm using various electric field models, Jordanova et al. (2006) found that the Volland-Stern model produced a plasmapause location closer to that identified from IMAGE EUV data than the model of Weimer (2001). The $K_p$-dependent version of the Volland-Stern model used by Jordanova et al. (2006) was derived using plasmapause observations to determine the strength of the convection (May-

nard and Chen 1975) and showed indeed very good agreement with IMAGE plasmapause observations.

### 2.3 Plasmasphere-Magnetosphere Coupling

In this section we discuss the influence of the plasmasphere on the excitation of electromagnetic ion cyclotron (EMIC) waves and precipitation of energetic ions in the inner magnetosphere. In the inner magnetosphere the cold plasmaspheric populations overlap spatially with high-energy plasma forming the ring current and the radiation belts. This is an environment suitable for the amplification of EMIC waves as first predicted by Cornwall et al. (1970) and subsequently investigated by many others (e.g., Anderson et al. 1992; Gary et al. 1995). Scattering by EMIC waves will lead to the precipitation of ring current ions and the excitation of subauroral arcs (Spasojević et al. 2004; Burch et al. 2005). Detached dayside proton arcs have been recently observed with the IMAGE Far UltraViolet (FUV) instrument as subauroral arcs separated from the main oval and extending over several hours of LT in the afternoon sector (e.g., Immel et al. 2002). To study the interplay of hot ring current ions with cold plasmaspheric material during the 23 January 2001 proton arc event, Jordanova et al. (2007) used their kinetic RAM coupled with the plasmasphere model of Rasmussen et al. (1993). The RAM solves numerically the bounce-averaged kinetic equation for the distribution functions of $H^+$, $O^+$ and $He^+$ ring current ions (from $\sim$100 eV to 400 keV) in the equatorial plane for radial distances from 2 to 6.5 $R_E$ and all MLT. Losses due to charge exchange, Coulomb collisions, atmospheric collisions at low altitudes, and drift through the dayside magnetopause are included (Jordanova et al. 1997). The growth rate of EMIC waves is calculated self-consistently by solving the hot plasma dispersion relation with ring current parameters and plasmaspheric densities obtained simultaneously from the coupled models; the wave amplitudes are calculated with an analytical expression derived on the basis of statistical studies. A plasmaspheric ion composition of 77 % $H^+$ , 20 % $He^+$ , and 3 % $O^+$ is assumed for these calculations (Young et al. 1977; Horwitz et al. 1981). Quasi-linear diffusion coefficients from Jordanova et al. (1996b) are used to calculate the pitch angle scattering of ring current ions into the loss cone due to resonant interactions with EMIC waves.

The evolution of equatorial plasmaspheric density, EMIC wave growth, and proton precipitation during 23–24 January 2001 is shown in Fig. 4. Wave-particle interactions are negligible if the integrated wave gain is below 20 dB (the wave amplitudes are below 0.1 nT). Geoeffective plasma waves are thus preferentially excited along the plasmapause or at larger $L$-shells in regions of enhanced plasmaspheric densities occurring within dayside drainage plumes. The EMIC wave excitation increased after fresh ion injections from the magnetotail and westward ion drift through the duskside magnetosphere. On 23 January 2001 the wave gain reached a maximum in the postnoon MLT sector at $L \approx 6$ between hours 47 and 48 (Fig. 4a), and vanished by hour 49 due to the wave scattering feedback and isotropization of the proton ring current. This indicates that enhanced plasmaspheric density (Fig. 4b) is only one of the factors needed for the excitation of EMIC waves, ring current proton anisotropy is another important factor. The RAM predicted weak proton precipitation from EMIC wave scattering beginning around hour 47 (Fig. 4c); its position matched the observed by IMAGE FUV equatorward edge of the auroral oval. By hour 48 the observed proton arc was well developed, and its projection onto the equatorial plane corresponded to the region of strong proton precipitation from EMIC wave scattering predicted with RAM. Note that in agreement with FAST (Fast Auroral SnapshoT) satellite data (Immel et al. 2002) the 10−40 keV precipitating fluxes were the strongest in the model (Jordanova et al. 2007), indicating

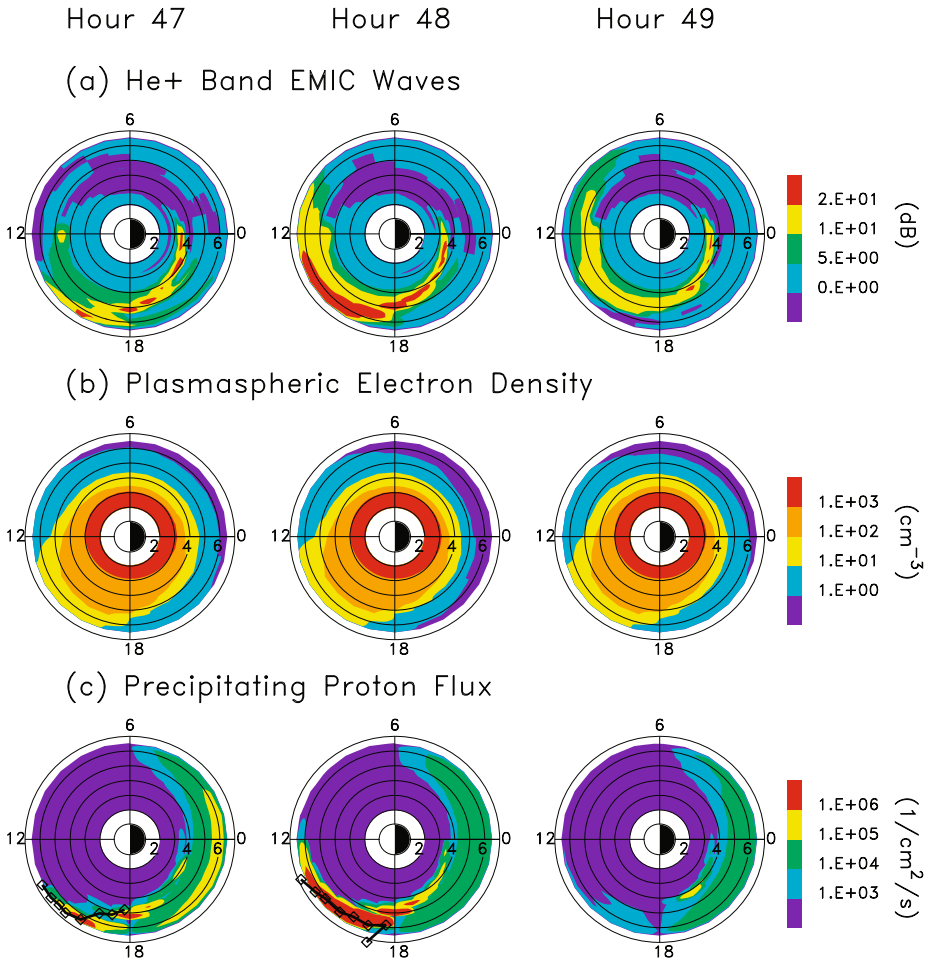


**Fig. 4** **a** Calculated wave gain (dB) of $He^+$ band (between $O^+$ and $He^+$ gyrofrequencies) EMIC waves as a function of radial distance in the equatorial plane and MLT at selected hours after 00:00 UT on 22 January 2001. **b** Equatorial plasmaspheric electron densities ($cm^{-3}$). **c** Precipitating 10−40 keV proton number flux (1 $cm^{-2}\,s^{-1}$); the *diamond line* indicates the low-latitude boundary of IMAGE FUV (Far UltraViolet) images of proton precipitation mapped to the solar magnetic (SM) equatorial plane using the Tsyganenko and Stern (1996) magnetic field model

that the proton arc emission was caused mainly by precipitating ions in this energy range. After hour 48 the observed proton arc receded to higher magnetic latitudes and the emission started to fade. There was no significant precipitation predicted by RAM at hour 49, in very good agreement with these observations. The study of Jordanova et al. (2007) showed the first comparisons of modeled proton precipitation with IMAGE FUV observations and demonstrated that scattering by EMIC waves is a viable mechanism for the generation of detached subauroral proton arcs.

## 3 The Kinetic Approach

### 3.1 Plasmapause Formation

The kinetic approach was also used to study the formation of the plasmapause by the mechanism of quasi-interchange instability (Lemaire 1985, 2001). This mechanism causes the peeling off of the plasmasphere as a result of sudden enhancements of the convection velocity associated with substorms in the night side. This enhanced azimuthal convection velocity leads to increased centrifugal acceleration in the outermost layers of the plasmasphere and a reduction of the total field-aligned potential barrier that ions have to overcome to reach the equatorial plane. This prompts the uplift of ions out of the underlying ionosphere. The enhancement of the field-aligned expansion velocity reduces the plasma density at high altitudes along all geomagnetic field lines traversing the zero-parallel force (ZPF) surface. This surface is the locus of points where the components of the gravitational and centrifugal acceleration balance each other in the direction parallel to the geomagnetic field lines. As a consequence of the plasma density diminution at high altitude along the field lines traversing the ZPF surface, a steep density gradient is formed into the plasmaspheric equatorial density profile. This steep plasma density gradient corresponds to a new plasmapause. It is formed where and when the azimuthal component of magnetospheric convection velocity is occasionally raised to values larger than the corotation velocity in the unperturbed core of the plasmasphere. This is how outer layers of the plasmasphere are peeled off and how plasma elements are detached according to the interchange theory for the formation of the plasmapause (Lemaire 2001).

The increased upward ionization flux which is prompted by the lowering of the field-aligned potential barrier depletes the mid-latitude ionosphere in the nightside MLT sector, where and when the eastward component of the convection electric field is suddenly enhanced. This leads to the formation of F-layer ionization troughs in the mid-latitude ionosphere as observed by Muldrew (1965) from ALOUETTE data. As an additional result of the upward $H^+$ and $He^+$ ions fluxes along all geomagnetic field lines beyond those which are tangent to the ZPF surface, the concentrations of these light ions are depleted, in both conjugate ionospheric regions. This is how light ion troughs (LIT) are developing beyond the projections of the ZPF surface at low altitudes in the ionosphere (Taylor and Walsh 1972). All these well documented events and features are observed following substorm events. According to Lemaire's theory for the formation of the plasmapause, they are consequences of the field aligned plasma distribution driven unstable by enhanced centrifugal effects at the innermost edge of substorm injection clouds (Lemaire 1974, 1985).

Dynamical simulations have been developed to determine the position of the plasmapause due to the erosion of the plasmasphere by the combined influence of the interchange instability and $K_p$-dependent electric field distributions (Pierrard and Lemaire 2004). The results predicted by models that include interchange have been compared with success to different IMAGE EUV observations during various periods of time including quiet periods, substorms and storms (Pierrard and Cabrera 2005, 2006; Pierrard 2006). The models predict an extended equatorial plasmasphere during prolonged quiet periods and plumes formation in the afternoon sector when the level of geomagnetic activity suddenly increases. Beside the sunward shift of the dusk-side plasmasphere during episodes of enhancement of the dawn-dusk component of magnetospheric convection electric field, an alternate mechanism of formation of such attached plasmatails or plumes was proposed by Lemaire (2000). Results of the interchange-included simulations have also been compared successfully with CIS (Cluster Ion Spectrometer) (Rème et al. 2001) and WHISPER (Waves of HIgh frequency

and Sounder for Probing Electron density by Relaxation) (Décréau et al. 2001) observations onboard CLUSTER by Dandouras et al. (2005), Darrouzet (2006) and Schäfer et al. (2007). Moreover, Schäfer et al. (2008) studied the spatio-temporal structure of a poloidal Alfvén wave near the dayside plasmapause based on CLUSTER observations of magnetic and electric fields.

The results of the dynamical simulations based on the inclusion of the interchange mechanism have been compared to the traditional MHD-based convection-only mechanism, in which the plasmapause location is determined dynamically under the influence of a time-dependent potential electric field. The axioms and assumptions of both mechanisms have been recalled in detail in a recent article by Lemaire and Pierrard (2008). The plasmapause positions predicted by these two alternative theories (i.e., convection only and convection plus interchange) have been determined numerically. They have been compared for different empirical electric field models described in this issue by Reinisch et al. (2008): Volland-Stern-Maynard-Chen (VSMC) model, McIlwain's E5D model, and Weimer's model. The predicted positions and overall shape of the equatorial plasmapause cross-section have been compared for these three different electric field models (Pierrard et al. 2008).

The predictions of both alternative kinds of simulations have been compared to whistler-derived densities and global images obtained by EUV, during several storm and substorm events. These simulations confirmed that the presumed plasmapause positions and shapes depend on the variation of the geomagnetic activity level during the preceding days and also on the magnetospheric convection electric field model. When the modeled plasmapause is determined by the combined influence of instability and convection, it is formed slightly closer to the Earth than with the convection only scenario. Plumes are formed in both scenarios and for all electric field models considered in Pierrard et al. (2008) study. Nevertheless, different features are obtained for the plasmasphere structure depending on the simulation scenario and electric field models which had been adopted.

Figure 5 illustrates the differences obtained for the equatorial position of the plasmapause with the different mechanisms (ideal MHD in upper panels, interchange in the bottom left panel) and with for all three electric field models at 21:00 UT, after the magnetic storm of 17 April 2002. The E5D, VSMC and Weimer are used in the three upper panels; only E5D is used in the bottom left panel. The IMAGE EUV observation of the equatorial plasmapause position at 21:07 UT is illustrated in the bottom right panel. VSMC and Weimer models produce a plasmapause closer to the Earth than E5D. In the midnight sector, VSMC and Weimer electric field models lead to a plasmapause position too close to the Earth compared to the EUV observations, while the plasmapause position obtained with E5D corresponds to the EUV observations in this midnight sector. In the noon sector, E5D reproduces EUV observations when the interchange is taken into account.

### 3.2 Plasmaspheric Wind

The distribution of cold plasma in the Earth's inner magnetosphere depends on the interplay between the corotation electric field, the convection electric field, and plasma instabilities. The corotation electric field is fairly stable but the convection electric field is unsteady and, therefore, the plasma distribution may vary substantially both in space and time during active periods. When there are disturbances in the solar wind, flux tubes outside the corotation region drain their plasma toward the magnetopause under the effect of the duskward convection electric field and a well-defined and sharp density gradient, the plasmapause, is observed. On the contrary, when magnetospheric convection is very weak for a prolonged period, the effect of the plasmasphere corotation with the Earth dominates up to large radial

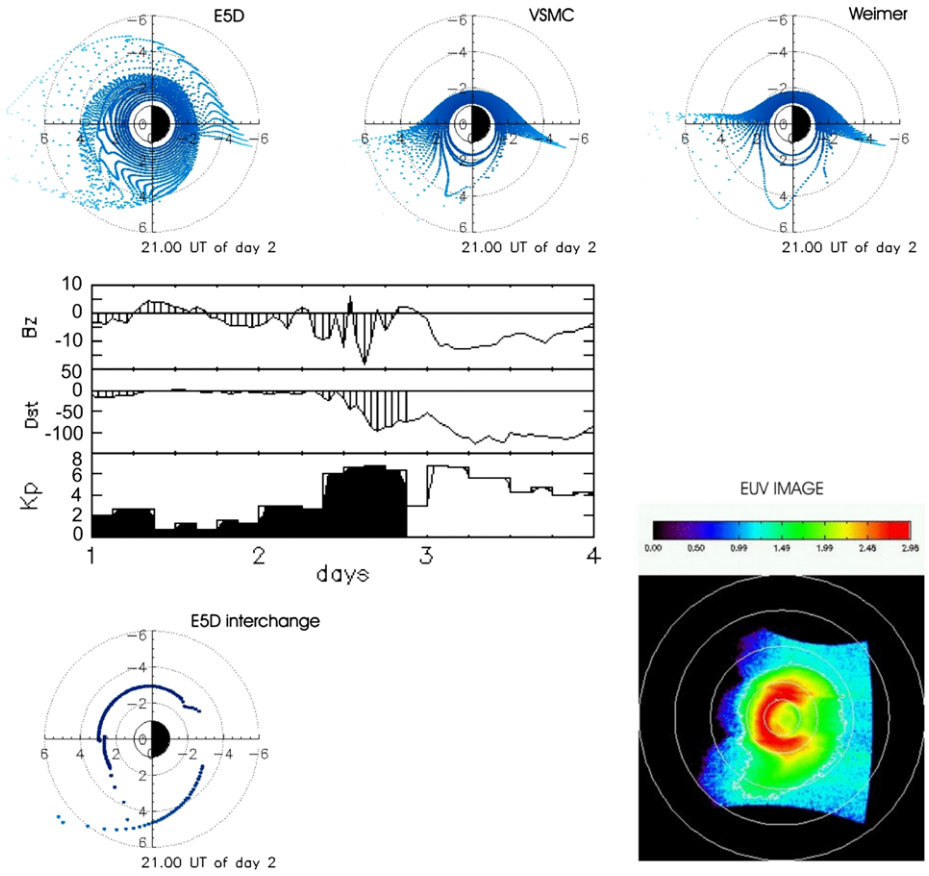


**Fig. 5** The equatorial cross section of the plasmasphere after the magnetic storm of 17 April 2002 at 21:00 UT. (*Upper panels*) MHD simulations with E5D (*left*), VSMC (*middle*), Weimer (*right*) electric field models. The $Z$ component of the interplanetary magnetic field (IMF) ($B_Z$), the disturbance storm-time index ($Dst$) and the geomagnetic activity index $K_p$ from 16 April 2002 0:00 UT up to 18 April 2002 24:00 UT are illustrated below the upper left panel. (*Bottom panels*) Interchange simulations with E5D (*left*) and observations of IMAGE EUV at 21:07 UT (*right*). The *white circles* correspond respectively to $L = 2$, 4, 6 and 8. (Adapted from Pierrard et al. 2008)

distances ($<7\ R_E$). The magnetic flux tubes inside the corotation region are supplied with plasma continually flowing up out of the ionosphere, and building up a smooth electron density transition from plasmasphere to the outer subauroral regions as observed RPI onboard the IMAGE spacecraft (Tu et al. 2007). Therefore, the plasmasphere is not always bounded by a steep density gradient as commonly believed.

Noting the systematic differences between theoretical hydrostatic models and the observed density distribution in the plasmasphere, Lemaire and Schunk (1992, 1994) suggested the conceptual existence of continual losses of plasma from the plasmasphere, a plasmaspheric wind, driven by interchange motions. They postulate the existence of a slow and permanent transport of plasma across the magnetic field from the inner to the outer regions of the plasmasphere, even during prolonged periods of quiet geomagnetic conditions when substorm disturbances are absent. This plasmaspheric wind is rather similar to that of the subsonic expansion of the equatorial solar corona. Such a radial plasma transport implies in-

deed that plasma streamlines are not closed, and, therefore, that cold plasma elements slowly drift outward from the inner plasmasphere to the plasmapause along winding up spiral drift paths.

### *3.2.1 The Role of Quasi-Interchange Modes*

From a theoretical point of view, the presence of a plasmaspheric wind has been considered to result from a plasma interchange motion driven by an imbalance between gravitational, centrifugal and pressure gradient forces.

Gold (1959) was the first to introduce the concept of interchange of magnetic flux tubes in the magnetospheric context. His so-called strict interchange assumes a one-to-one interchange between magnetic flux tubes enclosing the same magnetic flux and thus leaving the shape of the magnetic field lines unchanged as well as the magnetic energy of the system unperturbed. Cheng (1989) pointed out that this model is at odds with the requirement of total pressure balance, and that a realistic flux tube interchange must be accompanied by a change in field magnitude. The so-called generalized interchange model of Southwood and Kivelson (1987) still assumes that the interchanging flux tubes preserve everywhere the direction of the local magnetic field, but they relax the condition that the energy density of the magnetic field is unperturbed by the interchange. Both models are in fact unphysical, insofar as true interchange motions of plasma elements generally also entail distortions of the magnetic field that preserves the total pressure (plasma plus magnetic pressure). The presence of stratification of the plasmaspheric pressure distribution and of non-electromagnetic forces leads in fact to the destabilizing of a broader category of modes driven by buoyancy forces, known as quasi-interchange modes that trigger transverse as well as translational plasma motions (Newcomb 1961; Ferrière et al. 1999; André 2003; Ferrière and André 2003).

These modes can become unstable in the limit of small parallel wave vector, and fall into two types in the limit of zero parallel wave vector. The type 1 quasi-interchange mode or transverse interchange mode corresponds to plasma motions which are predominantly perpendicular to magnetic field lines and results in the exchange of plasma elements across magnetic field lines. The type 2 quasi-interchange mode or translational mode corresponds to motions of the plasma predominantly along flux tubes.

### *3.2.2 Testing the Instability Criteria of Quasi-Interchange Modes in the Plasmasphere*

André and Lemaire (2006) tested the local stability of quasi-interchange modes for various diffusive and exospheric hydrostatic field-aligned density distributions expected to be representative of the equatorial regions of a saturated plasmasphere under very quiet geomagnetic conditions. When the only effect of the centrifugal force due to corotation of the plasma with the angular velocity of the Earth is taken into account, the corotating plasma appears convectively stable inside geosynchronous orbit. However, when the magnetic curvature of the magnetic field lines is properly taken into account, the conclusions obtained in the case of straight field lines are significantly altered since the magnetic curvature is found to have a much larger influence than the effective gravity (including the effect of the centrifugal force) in the Earth magnetosphere. The thermal plasma confined in the Earth's dipole magnetic field cannot remain in magnetostatic equilibrium but becomes convectively unstable much deeper inside the equatorial plasmasphere, at $R = 2\,R_E$ and beyond. The type 2 quasi-interchange or translational mode appears to play a more important role than the type 1 quasi-interchange or transverse mode. The type 2 mode appears unstable inside

the geosynchronous orbit for $R < 6.6\ R_E$ both in the case of a diffusive equilibrium (DE) model (Lemaire 1999) and in the case of Pierrard and Lemaire (2001) exospheric model for $R > 2.3\ R_E$. Since the latter model fits the empirical equatorial density distribution of Carpenter and Anderson (1992), the later conclusion holds also in that case. Similar conclusions are obtained with other empirical models characterized by larger density gradients (e.g., Reinisch et al. 2004). The existence of a static equatorial plasmasphere seems therefore to be questionable, even in a saturated stage following a long period of quiet geomagnetic conditions.

### *3.2.3 Implications of a Plasmaspheric Wind and Future Refinements*

Although the type 2 quasi-interchange or translational mode is considered primarily to lead to plasma motions parallel to the magnetic field line, it should be pointed out that it does not imply strictly parallel motions: The motion necessarily acquires also a transverse component (Ferrière et al. 1999). In that sense, this would be compatible with the concept of plasmaspheric wind introduced by Lemaire and Schunk (1992), consisting of a slow and permanent cross-$B$ transport of plasma from the inner to the outer equatorial regions of the plasmasphere accompanied by a field-aligned upward ionization flow.

Both the diffusive and exospheric models used by André and Lemaire (2006) are oversimplified models, since they assume the plasma distribution to be stationary, i.e., time-independent and with no net mass flow along magnetic field lines, whereas for example asymmetries in the geomagnetic field line geometry and in the boundary conditions at the feet of the flux tube are expected to lead to dynamic inter-hemispheric plasma flows. Their application suffers from large uncertainties due to the use of various simplifying assumptions but interesting conclusions can be drawn from their simplified formulation. Further refinements of their application will have to include, in particular, the coupling of low-energy and high-energy plasma in the plasmasphere, the ionospheric effects arising at the foot of the flux tubes, as well as the observed plasma corotation lag (Burch et al. 2004).

In a recent comparison of measured radial abundance profiles from EUV observations with predicted profiles from the Sheffield University Plasmasphere Ionosphere Model, SUPIM (Bailey et al. 1997) during a period of quiet geomagnetic activity, Sandel and Denton (2007) noted some disagreement between this model and the EUV observations beyond $R = 4\ R_E$ that are possibly a signature of physical processes not accounted for in the model. A plasmaspheric wind is one possible process whose inclusion in future magnetospheric convection models might resolve the model-observation disagreement. Recent analysis of cold ion measurements obtained in the plasmasphere by CIS onboard CLUSTER may have provided the first experimental confirmation of such a plasmaspheric wind (Dandouras 2008; Darrouzet et al. 2008, this issue).

## 3.3 Transport of Plasmaspheric Material Caused by Ultra Low Frequency Waves

The study of transport of plasmaspheric material in plumes is not only important to understand the plasmasphere dynamics but also to understand the physics of the magnetic reconnection at the magnetopause (Borovsky and Hesse 2007). The presence of dense plasma modifies the local reconnection rate by lowering the Alfvén velocity. Some escaping particles could subsequently move toward the magnetotail and subsequently be recirculated into the inner magnetosphere during substorms. Thus the formation of plumes is of vital importance if we are to understand the mass budget in near-Earth space (Chappell et al. 1987).

The formation of a plasmaspheric plume is often discussed in terms of global plasma transport during times of large geomagnetic activity such as substorms and/or storms (Grebowsky 1970; Elphic et al. 1996) including cases with IMF directed southward (negative $B_Z$) (Goldstein et al. 2002; Chen and Moore 2006). However, observations during quiet and moderate periods of cold plasma in the afternoon sector, well outside the nominal plasmasphere have remained puzzling (Chappell 1974; Carpenter et al. 1993; Matsui et al. 1999; Yoshikawa et al. 2003). Are these cold plasma regions residual density features that linger long after the recovery after storms and substorms? An alternate explanation involves ULF waves, which are often excited by the variation of the solar wind dynamic pressure (e.g., Farrugia et al. 1989) and/or by the velocity shear at the magnetopause (e.g., Engebretson et al. 1995). All current electric field models include a flow stagnation point somewhere on the duskside, where $\boldsymbol{E} \times \boldsymbol{B}$ drifts are weak. At this stagnation point (and possibly in a large area on the duskside during quiet conditions), the wave field might exceed the background field, and thus could dominate cold plasma transport. This idea, suggested by Carpenter and Lemaire (2004) as part of the proposed plasmasphere boundary layer (PBL) concept, could help explain the prevalence of cold plasma at large $L$ values in the afternoon sector even during extended quiet conditions. Chen and Wolf (1972) considered time variable electric fields but with longer time scale (8 hours) than ULF waves. Grebowsky and Chen (1976) considered a case applying spatially variable electric fields to examine transport of plasmas. Recently, Adrian et al. (2004) simulated ULF waves related to the formation of radially bifurcated plasmaspheric features.

Matsui et al. (2000) considered this problem with temporally variable electric fields. In this study, a test particle simulation was performed in an idealized mathematical model to examine whether ULF wave fields could cause cold plasma to be transported to the magnetopause. The background electric potential $\Phi$ in the inertial frame is given by Volland-Stern model (Volland 1973; Stern 1975) without ionospheric shielding:

$$\Phi = \frac{C_1}{L} - C_2 L \sin\phi, \tag{1}$$

where $C_1$ is a constant to specify the size of the corotation potential, $L$ is the value of McIlwain's parameter, $C_2$ is a variable to specify the intensity of the dawn-dusk electric field component, and $\phi$ is the MLT expressed in radians. In addition, the wave electric potential $\Delta\Phi$ defined by the following equation is added:

$$\Delta\Phi = a \cdot \exp(-br^2) \cdot \sin\left(\frac{2\pi t}{T}\right), \tag{2}$$

where $a$ is the wave amplitude, $b$ is the spatial size of the wave potential taken as $1.0 \times 10^4\ {R_E}^{-2}$, $r$ is the distance from the stagnation point, $t$ is time, and $T$ is the wave period, taken as 300 s. It is assumed that there is no magnetic field perturbation, which is true for the fundamental mode of standing Pc 5 waves. These waves have a typical period of ~300 s. The location of the stagnation point is set at $L = 6$ and 18:00 MLT. The particle orbit without perturbation is traced from 15:00 MLT, which leads to the location $L = 5.99$ at 18:00 MLT. The orbit is traced by a Runge-Kutta method with a time step of 0.5 s.

The orbit around the stagnation point is shown in Fig. 6a. This orbit is inside the last closed equipotential (LCE) and rotating around the Earth, although the period is 55.9 hours, longer than 1 day due to a finite convection electric field in the vicinity of the stagnation point. It should be noted that this model is not based on physical processes but mathematical because the calculation relies on the existence of a singular mathematical point. Moreover,

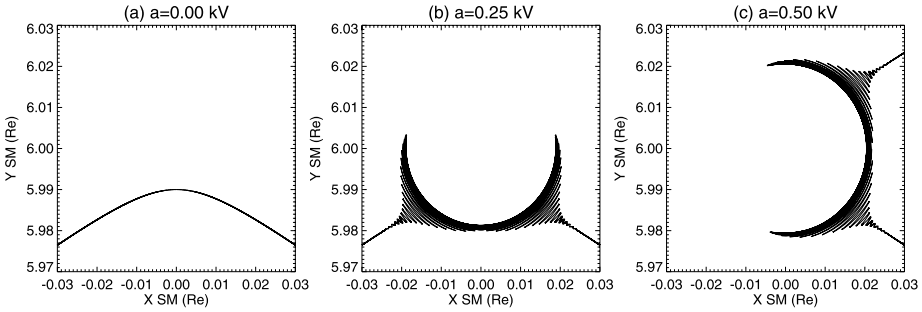


**Fig. 6** Particle orbits around the stagnation point $(X, Y)_{SM} = (0.00, 6.00)\, R_E$ with amplitudes of wave potential: **a** $a = 0.00$ kV, **b** $a = 0.25$ kV, and **c** $a = 0.50$ kV

the wave field essentially assumes coherent waves, which is not necessarily a good description of the turbulence that exists. When a perturbed potential $\Delta\Phi$ with $a = 0.25$ kV is added, the particle orbit starts to deviate at a distance $\sim$0.02 $R_E$ from the stagnation point (Fig. 6b). In this case, the perturbation is not large enough to shift the particle orbit from a closed to an open one. After passing near the stagnation point under the influence of waves, the orbit returns to the same as that without perturbation. The orbit is further modified when a larger wave potential $a = 0.50$ kV (Fig. 6c) than the previous case (Fig. 6b) is specified. In this case, the particle orbit is transferred from the original closed orbit to the open orbit and is subsequently transported toward the magnetopause.

The above simple simulation demonstrates that the behaviour of plasmaspheric particles, in particular whether they remain on closed drift paths or are carried toward the magnetopause, can depend on the wave amplitude at the stagnation point. It is often reported that the wave amplitude is comparable to or larger than the background field from various observations such as Equator-S (Quinn et al. 1999), Geotail (Matsui et al. 2000), CLUSTER (Matsui et al. 2003), and LANL geosynchronous satellites (Goldstein et al. 2004). At the stagnation point itself (where the DC electric field is, by definition, zero), the wave component dominates.

In reality, the wave amplitude will not be constant as assumed in the above simulation. LeDocq et al. (1994) reported turbulent behaviour of the density variation, one behaviour expected in the PBL. If this is the case for the electric field variation, the particles at times may be transported to the magnetopause under the dominating influence of ULF waves, and at other times may not. Another open question is the relative importance of this ULF-related mechanism relative to other known mechanisms such as SAPS (Foster et al. 2004), the interchange instability mechanism (Pierrard and Lemaire 2004), or global fields from storms or substorms. Under various conditions, duskside plasma transport could result from various different combinations of the above-mentioned mechanisms.

Finally, it is worth pointing out that the above simulation ignores inductive electric fields created by magnetic variation, and assumes that (barring wave fields) the dominant influence is $\boldsymbol{E} \times \boldsymbol{B}$ drift. This latter assumption rules out the possible dominance of the interchange instability or curvature drift (André and Lemaire 2006), which might especially be true near the stagnation point in the $\boldsymbol{E} \times \boldsymbol{B}$ field. Ideally, future simulations that include realistic, self-consistent electromagnetic fields (with treatments of all possible mechanisms) would be best suited for comparing the relative importance of the various mechanisms.

### 3.4 Electric Field in Equilibrium Theory

The first studies of the field aligned plasma distribution in an ion-exosphere considered the case of diffusive equilibrium (DE), in which the plasma velocity distribution function (VDF) is Maxwellian and isotropic (Bauer 1962). The latter studies envisaged the case of exospheric equilibrium (EE), in which the velocity distribution is anisotropic, but without any net inter-hemispheric flow.

Due to the large mean free path compared to the gyroradius of charged particles, they can move longer distances along magnetic field lines than in the direction perpendicular to the magnetic field $\boldsymbol{B}$. This implies that the motion of charged particles is determined in a co-moving frame of reference where the $\boldsymbol{E} \times \boldsymbol{B}$ convection velocity is null. Except during transient flow regimes where electrostatic shocks may be able to propagate downwards or upwards, the plasma density is distributed in a smooth manner along plasmaspheric flux tubes.

When the distribution of plasma is in hydrostatic equilibrium, its field aligned density distribution is determined by the gravitational potential. But besides the gravitational forces, which are proportional to the ion or electron masses, there is always an additional internal force due to a polarization electric field: the Pannekoek-Rosseland electric field (Lemaire and Gringauz 1998). This electric field has non-zero components both perpendicular and parallel to the magnetic field lines. This polarization field exists in all geophysical and astrophysical plasmas as a result of the charge separation created by the difference between the gravitational forces acting on the electrons and on the heavier ions.

Note that when the plasma is not in hydrostatic equilibrium but has a bulk motion upward or downward (across or along magnetic field lines), the inertial force produces another polarization electric field in addition to the Pannekoek-Rosseland component. Sheared convection velocity distributions, like that existing along magnetic flux tubes in the plasmaspheric wind, creates an additional electric field component, which also has a non-zero parallel component such that $\boldsymbol{E} \cdot \boldsymbol{B} \neq 0$. The existence of parallel electric field components in sheared convection velocity distributions has been discussed and modeled by Echim and Lemaire (2005) in the context of plasma elements impulsively injected across the magnetopause. The parallel components of polarization electric fields play also a basic role in interchange motion (Gold 1959) and quasi-interchange motion in magnetospheric plasmas (Newcomb 1961; André 2003; André and Ferrière 2004).

The parallel component of polarization electric fields is of the order of $\mu\mathrm{V\,m^{-1}}$, which is much smaller than the perpendicular component of magnetospheric convection or of the corotation electric fields ($\mathrm{mV\,m^{-1}}$), in a fixed inertial frame of reference. The convection and corotation electric fields can be reduced to zero, by changing the frame of reference in which it is measured (by a Lorenz transformation), while this is never the case for the (small) parallel component of $\boldsymbol{E}$. The relative "smallness" of the parallel electric fields (when compared with the convection electric field intensity) should not be considered as a reason to ignore its effect, nor to justify the postulate that $\boldsymbol{E} \cdot \boldsymbol{B} = 0$ everywhere along geomagnetic field lines (Parks 2004).

### 3.5 Stationary Density Distribution in the Plasmasphere

The centrifugal effects also influence the field-aligned distributions of ions at high altitudes. The centrifugal effect tends to increase the DE densities of ions and electrons at highest altitudes. For $L > 5.78$, the increase of the equatorial number density is very significant when the corotation of the plasmasphere is taken into account. A significant amount of cold

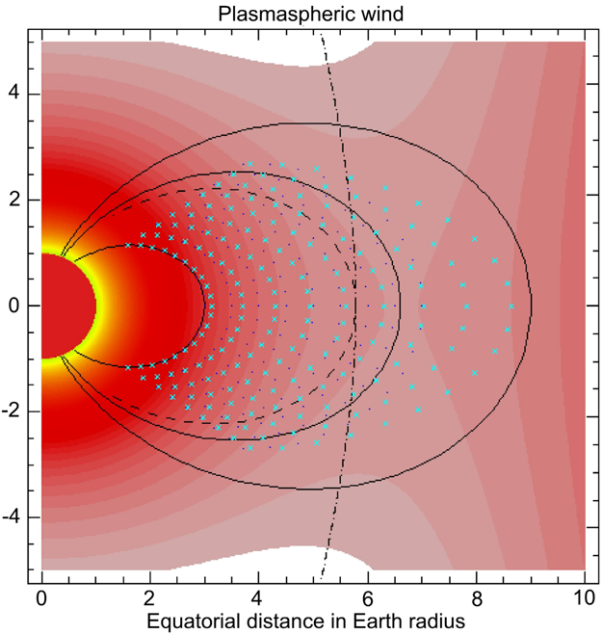


**Fig. 7** Number density of a kinetic Maxwellian DE model. Above the ZPF surface located at $L = 5.78\ R_E$ for plasma corotation (*dot-dashed line*), the plasma density distributions become unstable. The *blue crosses* represent plasma elements displaced from their initial positions originally aligned along the dipole magnetic field lines, due to quasi-interchange plasma motion of type 2 driven unstable by the curvature of geomagnetic field lines

ionospheric plasma can then accumulate in the equatorial potential well beyond the ZPF surface, i.e., the surface where the field aligned components of the gravitational force and pseudo-centrifugal force balance each other.

This accumulation is illustrated in Fig. 7 where the DE equatorial density has a minimum at geostationary orbit: $R = 6.6\ R_E$. Beyond this radial distance, the DE density distribution tends to infinity. Since this situation is physically untenable, it must be concluded that the theoretical DE distribution of corotating plasma is convectively unstable. A theoretical accumulation of plasma in the equatorial region can be held off by the continuous radial outward flow of the plasmaspheric wind already discussed above and evacuating the plasma in excess. This excess of plasma is transported away by quasi-interchange plasma motion of type 2 driven unstable not only by the centrifugal effect but mostly by the effect of magnetic tension resulting from the curvature of geomagnetic field lines (André and Lemaire 2006). This sheared convection velocity, the plasmaspheric wind, is illustrated in Fig. 7 showing the displacements of plasma elements (the blue x symbols) from their initial positions (the black dots initially aligned along the dipole magnetic field lines which are represented by the solid lines in Fig. 7).

The amplitude of these unstable type 2 quasi-interchange displacements is largest close to equatorial plane, while the upward field aligned ionization flow out of the ionosphere maximizes at low altitude along the geomagnetic field lines. This plasmaspheric flow is illustrated in an animation available on the Internet,[1] together with other animations of plasmaspheric wind and plasmapause formation.

Although various other field-aligned electron density distributions have been proposed in the analysis of whistler frequency-time spectrograms, DE models were usually adopted for field lines located inside the plasmasphere. In such DE models, the slope of equatorial

[1] http://www.aeronomie.be/plasmasphere/plasmaspherewindsimulation.htm.

density distributions gradually decreases with radial distances and tends to zero at 6.6 $R_E$. However, the slopes of the equatorial ion density profiles measured by OGO-5 are consistently steeper than the theoretical prediction of the DE models. This led Lemaire and Schunk (1992, 1994) to suggest the existence of the plasmaspheric wind. The inadequacy of DE models to describe the plasma distribution inside the plasmasphere is not only demonstrated by the theoretical evidence, but also from an experimental stand point by WHISPER observations onboard CLUSTER (Darrouzet et al. 2008, this issue), as well as by IMAGE RPI observations (Tu et al. 2004).

### *3.5.1 The Exospheric Equilibrium Density Distributions*

Outside the plasmasphere, the density is more than one order of magnitude smaller than inside the plasmasphere itself, i.e., less than 50 electrons and ions per $cm^{-3}$ at $L = 4$ in the equatorial plane. The free flight time needed for a 0.2 eV proton to move along an $L = 4$ field line from one hemisphere to the conjugate one is 2 hours, if it has not been deflected by Coulomb collisions or wave-particle interactions along its spiraling trajectory (Lemaire 1989). The cumulative number of collisions during their flight from one hemisphere to the other is almost the same for the thermal electrons and $H^+$ ions (Lemaire 1985, 1989). Therefore, the thermal plasma can be considered as nearly collisionless in the plasmatrough above an altitude of 1000 km, as well as in plasmaspheric flux tubes during the early stages of refilling phases.

Let's assume that the background plasma density has been reduced to low values in the plasmatrough, after a peeling off event and the formation of a new plasmapause closer to the Earth. Under these transient conditions, the thermal protons and electrons of ionospheric origin can move rather long distances along magnetic field lines without being significantly deflected. Their orbits can be organized into various classes (Lemaire 1976, 1985). These classes are: (e) "escaping" particles, which have enough kinetic energy to go over the total potential barrier; (b) "ballistic" particles, which do not have enough energy to do so; they fall back into the ionosphere. There are also four subclasses of trapped particles ($t_1, t_2, t_3, t_4$) which have mirror points either in the same hemisphere or in both hemispheres, and those which are trapped in the equatorial potential well for field lines with $L > L_c$ where $L_c = 5.78$. The latter $t_3, t_4$ classes do not exist for $L < L_c$.

When all these orbits are populated by ions and electrons whose velocity distributions functions are, for instance, Maxwellian and isotropic, the field-aligned density distribution corresponds to the DE model discussed above. Such an ideal state of equilibrium, corresponding to detailed balance between the particles of all these different classes, was assumed to be maintained by Coulomb collisions inside the plasmasphere. However, when one of these classes of orbits is un-saturated (i.e., when for instance the $t_3, t_4$ trapped particles are missing or under-populated) Coulomb pitch angle scattering will tend to deflect escaping particles as well as trapped particles to fill up the un-saturated classes of orbits. The pitch angle scattering process by Coulomb collisions could be enhanced by the effect of wave-particle interactions, provided that the spectrum of waves and their polarization are adequate and continuously regenerated to feed these additional pitch angle scattering mechanisms; there is not yet definite experimental evidence that this is indeed the case in the plasmasphere and plasmatrough.

The first collisionless (exospheric) models for the plasmasphere were developed by Eviatar et al. (1964). Lemaire (1976, 1985) worked out the effect of corotation on the field aligned distribution of thermal ions and electrons, assuming a Maxwellian VDF and empty classes of trapped particles. These kinetic models are labeled EE models.

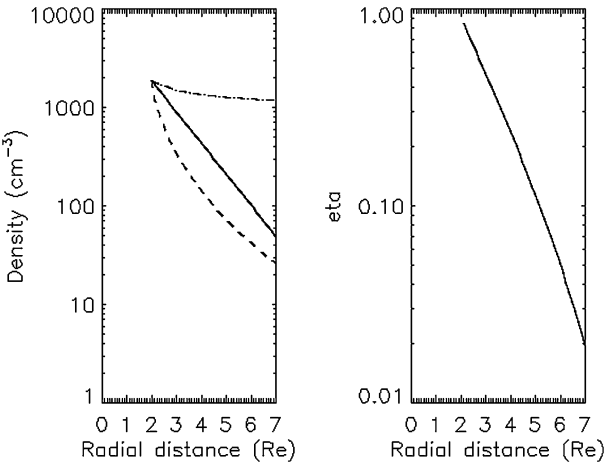


**Fig. 8** (*Left*) Equatorial density profiles in the plasmasphere obtained by Carpenter and Anderson (1992) from ISEE observations (*thick straight line*). The corresponding equatorial density profiles for DE (*upper line*) and EE (*lower line*) with Kappa distributions with $\kappa = 10$ are shown for comparison. (*Right*) Fraction *eta* of trapped particles to add to minimum exospheric models ($\kappa = 10$) to recover density profile from (Carpenter and Anderson 1992) corresponding to prolonged quiet magnetic conditions. (Adapted from Pierrard and Lemaire 2001)

A further extension of EE models has been developed by Pierrard and Lemaire (1996) for Lorentzian VDF instead of Maxwellian ones. The tails of the Lorentzian VDF are controlled by a parameter kappa: When kappa is small, there are a large number of suprathermal particles in the tail of the distribution. Conversely, the Lorentzian VDF becomes indentically Maxwellian when the kappa index tends to infinity. Figure 8 (left panel) illustrates equatorial plasmaspheric density profiles for a Lorentzian VDF with a high value of the kappa index. The upper dashed-dotted line in Fig. 8 (left panel) corresponds to the equatorial number density profile in case of DE. The VDFs of the electrons and protons are assumed to be Lorentzian with $\kappa = 10$ and isotropic (Pierrard and Lemaire 2001). Contrary to the DE models with Maxwellian VDFs for which the temperatures of the electrons and ions are uniform, DE models with Lorentzian VDFs have temperatures increasing with altitudes. Positive temperature gradients were first observed in the plasmasphere by Comfort (1986, 1996) and confirmed by the observations in Kotova et al. (2002) and Bezrukikh et al. (2003).

The lower dashed line in Fig. 8 represents the equatorial density corresponding to EE. In this case, the proton density is formed only of ballistic (b) and escaping (e) particles emerging from below the exobase level. In this model, no trapped particles with mirror points above the exobase are assumed to be present in the ion-exosphere.

The EE distribution can ideally be considered as a sort of minimum density model. Indeed, densities below the values predicted by EE models cannot be maintained much longer than one free flight time of ionospheric ions moving from one hemisphere to the other. Along field lines $L = 4$, this flight time is 2 hours for a proton of 0.2 eV while at $L = 6$ it is four hours (Lemaire 1985, 1989). For example, starting with a hypothetically void magnetospheric flux tube, after four hours the proton density distribution would have recovered to values equal or larger than those corresponding to the EE model. Therefore, EE models or the corresponding distribution obtained for a Lorentzian VDF (Pierrard and Lemaire 1996) are minimum models. They should be considered as initial boundary conditions in dynamical plasmaspheric refilling models like those proposed by Krall et al. (2008) and others. At any time between peeling off event and the long term saturation time, the field-aligned density distributions should be somewhere in between the two extreme EE and DE models.

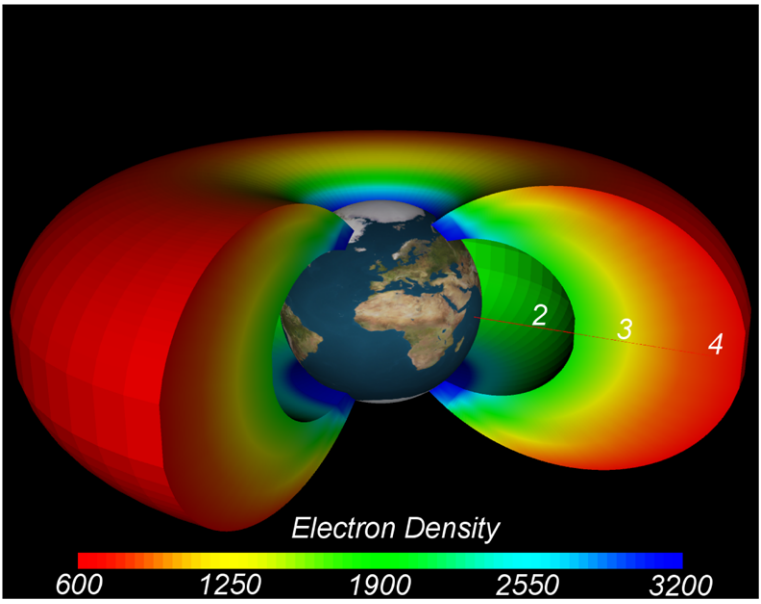


**Fig. 9** Kinetic model of the plasmasphere in three dimensions obtained by assuming a fraction of trapped particles so that the geomagnetic equatorial profile corresponds to ISEE observations. The electron density is given in $cm^{-3}$. (Adapted from Pierrard and Stegen 2008)

### *3.5.2 Physics Model Constrained by Empirical Data*

Pierrard and Lemaire (2001) constructed an intermediate stationary kinetic model of the plasmasphere, where $\eta$, the relative abundance of trapped protons and electron populations, was neither equal to 1 as in the DE model, nor null as in the EE model. In this intermediate kinetic model, $\eta$ is assumed to be a function of $L$, or of the invariant latitude of the dipole field lines. The values of $\eta(L)$ have been adjusted to recover the statistical equatorial electron density distribution obtained by Carpenter and Anderson (1992) from ISEE observations after prolonged quiet conditions. This observed equatorial density profile is represented by the thick straight line on the left panel of Fig. 8. The right panel of Fig. 8 illustrates how the relative abundance of trapped particles decreases with $L$ in order to recover the Carpenter and Anderson (1992) plasmaspheric density profile in the equatorial region.

It can be seen from the right hand side panel that the required relative fraction of trapped particles, $\eta(L)$, is smaller along the outermost field lines of the plasmasphere, than along the inner region flux tubes, where the average density is larger and consequently where pitch angle scattering of ballistic and escaping particle onto trapped orbits is most efficient.

This stationary kinetic model of plasmaspheric density distribution has recently been extended in three dimensions by Pierrard and Stegen (2008) to also simulate the density distribution outside plasmasphere and in the PBL. This more recent model of the plasmaspheric density distribution is also a function of the level of geomagnetic activity as determined by the $K_p$ index and is illustrated in Fig. 9. This model is in good agreement with satellite measurements, and especially with recent observations of IMAGE and CLUSTER (Pierrard and Stegen 2008).

## 3.6 Kinetic Process of Plasmaspheric Refilling

In a qualitative refilling scenario proposed by Lemaire (1985, 1989), ballistic and escaping particles from the ionosphere enter empty flux tubes. In less than 4 hours a field-aligned density distribution exceeding that of the EE model is set up along all refilling flux tubes. These ionospheric particles build up a dynamical field-aligned density distribution like that studied in the dynamical refilling model of Krall et al. (2008). The pitch angle distribution of the ions is expected to be initially strongly anisotropic and peaked in the field-aligned direction, i.e., confined to the source and loss cones. For larger pitch angles, corresponding to trapped particles, reduced phase space density are expected during the early phase of the refilling process. However, since Coulomb collision rate is never equal to zero and since it increases rapidly when the total flux tube content increases, the density in the flux tubes is expected to increase rapidly due to the continual accumulation of trapped particles by Coulomb pitch angle scattering and wave-particle interactions.

As time passes, more and more ballistic and escaping particles are scattered onto trapped orbits at larger pitch angles. The particles of lowest energies (subthermal) will be scattered more quickly than the suprathermal ones. Indeed, the Coulomb collision cross section is a rapidly decreasing function of the relative speed between colliding charged particles. Therefore, it is expected that the pitch angle distribution of particles with the lowest energies will become isotropic first. Later on, the pitch angles distribution of suprathermal particles also become more isotropic (Lemaire 1989). The evolution of the pitch angle distribution from a cigar-shaped one to a more isotropic one should take place over a much shorter time scale for the electrons than for the protons of comparable energies.

### *3.6.1 Coulomb Collisions*

Fundamental progress has been done to describe the changes of the particle velocity distribution of the ions in the transition region between the collision dominated ionosphere and the collisionless ion-exosphere. This effort was led by Barakat et al. (1990, 1995), Wilson et al. (1992, 1993) and Barghouthi et al. (1993, 2001). These basic advances in the kinetic theory of the polar wind and post-exospheric models for plasmaspheric refilling are based on Direct Monte-Carlo Simulation method (DMCS); hybrid/semi-kinetic models, fluid/hydrodynamic models and particle-in-cell methods; numerical solutions of the kinetic Fokker-Planck equation have been proposed by Lie-Svendsen and Rees (1996), Pierrard (1996), Pierrard and Lemaire (1996, 1998), Pierrard et al. (1999) and Lemaire and Pierrard (2001). Tam et al. (2007) have recently reviewed the kinetic models of the polar wind.

Monte Carlo simulations of the effect of Coulomb interactions on the velocity distribution function of ionospheric ions streaming in an empty ion-exosphere have been investigated by Barakat et al. (1990) and by Barghouthi et al. (1993). These simulations have demonstrated that, at the exobase, where the mean free paths of $H^+$ ions become equal to the plasma density scale height, their velocity distribution function changes drastically from a nearly isotropic Maxwellian (in the collision dominated region) to one that is anisotropic and resembles a "kidney bean embedded in a Maxwellian". Barghouthi et al. (2001) generalized their Monte Carlo simulations to Lorentzian VDFs.

The quantitative DMCS results were confirmed and expanded by Wilson et al. (1992) using a hybrid particle-in-cell model to describe the gradual plasmaspheric refilling process. The plasma accumulation at high altitudes occurs through collisional thermalization and pitch angle scattering controlled by the rate of velocity dependent Coulomb collisions.

Just like Barghouthi et al. (1993), Wilson et al. (1992, 1993) determined the velocity space distribution, $f(v_\parallel, v, t)$ for the ions beams. Although different numerical methods

were used in both independent studies, they reached basically the same physical conclusions. Within a few hours after the refilling has started, a significant number of ions from the northern hemisphere return after reflection in the southern hemisphere and vice versa. The gap in phase space between the two counter streaming beams gradually fills from the ionosphere toward the equator. This is due to particles, which are scattered onto trapped trajectories by collisions, with the result that their mirror points has a 50% chance to jump up to higher altitudes getting further removed from the topside ionosphere. Most of these collisions occur at lower altitudes. When the gap is completely filled, the pitch angle distribution has a maximum at 90°. This occurs after about 34 hours for $L = 4.5$.

During the refilling process, the density decreases smoothly toward the equator where the plasma density is minimum, and there is no sign of propagating shock waves. Therefore, according to the kinetic and semi-kinetic or hybrid scenarios proposed, plasmaspheric refilling occurs from the base of the flux tube, and not from top to bottom.

Miller et al. (1993) have modeled field-aligned plasma flows in the plasmasphere using a one-dimensional hybrid particle code to study the interactions between upflowing thermal ions from conjugate ionospheres. They point out that self-consistent modeling of ionosphere-plasmasphere coupling is important and requires information down to an altitude of 200 km. Their kinetic simulations demonstrated that magnetospheric convection and particle injection can change the initial conditions for plasmaspheric refilling on timescales shorter than one hour. But over long timescales (days), this short timescale information is lost.

### *3.6.2 Monte Carlo Simulations*

The effects of magnetic field line divergence and of the external body forces were simulated separately in the study of Barghouthi et al. (1993). In subsequent Monte Carlo simulations, Barakat and Barghouthi (1994) examined the effect of wave-particle interactions on the velocity distribution of polar wind $H^+$ and $O^+$ ions flowing out of the ionosphere along magnetic field lines (Barakat et al. 1995). Effects of wave-particle interactions on Lorentzian VDFs were analyzed in Pierrard and Barghouthi (2006). More recently, Barghouthi et al. (2007) analyzed also the effect of finite electromagnetic turbulence wavelength on the high-altitude and high latitude $O^+$ and $H^+$ outflows. Barghouthi et al. (2008) showed that altitude and velocity dependent wave-particle interactions lead to the formation of toroids at high altitude for the ion VDFs.

Monte-Carlo simulations have also been employed by Yasseen et al. (1989) and Tam et al. (1995) to determine the velocity distribution of photoelectrons (treated as test particles) moving through a background of $H^+$, $O^+$, and the bulk of thermal electrons, which all participate in a current-free polar wind type ionization flow. In their latest hybrid simulation, the evolution of velocity distributions of the $O^+$ and $H^+$ are also determined by the Monte-Carlo method, while the bulk of thermal electrons is treated as a fluid. Their results agree with observations in various aspects. They demonstrate that a temperature anisotropy develops between upwardly and downwardly moving electrons. They find that upward moving photoelectrons produce an upward heat flux for the total electron population.

Although these Monte-Carlo simulations demand large amounts of CPU-time, they are rather illuminating and useful to test numerical models, which were developed by Lie-Svendsen and Rees (1996) and Pierrard and Lemaire (1998). Both obtain numerical solutions of the Fokker-Planck equation for the $H^+$ ion velocity distribution moving along diverging magnetic field lines in a background of $O^+$ ions. Both teams of investigators obtained independently solutions of the Fokker-Planck equations, which are similar to those

of the Monte Carlo simulations, although they employ different boundary conditions at the bottom of the transition layer, as well as different mathematical methods: Lie-Svendsen and Rees (1996) use the finite difference method, while Pierrard and Lemaire (1998) employ a generalized spectral method.

These numerical tools will enable the development of future post-exospheric approximations for ion velocity distributions, which are especially needed in the transition layers between the collision dominated ionosphere and collisionless magnetosphere. Novel numerical methods of this kind, including the Monte Carlo simulation and particle-in-cell method, have opened the door to modern plasma kinetic treatment of plasmaspheric, polar wind and magnetospheric modeling. They are nicely complementing the fluid, moments, and MHD approximations used for decades in space plasma transport theories (see the review by Fahr and Shizgal 1983).

## 4 Comparison Between MHD and Kinetic Approaches

Numerous theoretical models describing the outflow of ionospheric plasma at polar and mid-latitudes have been based on numerical integration of hydrodynamical transport equations or moment equations. Unlike the case of kinetic models, where plasma is described by the velocity distribution functions of its different particle species, in hydrodynamical models the plasma is described in terms of the total number density or of the partial density of the electrons and different ion species, of their bulk speeds, parallel and perpendicular temperatures, parallel and perpendicular heat flow tensor components or in terms of moments of higher order of the velocity distribution function.

In fluid models, the spatial distributions of these macroscopic quantities ($n_i$, $v_i$, $T_i$ ...) are obtained by solving the moment equations for each particle species. These moment equations are obtained by multiplying the Boltzmann equation by various velocity moments and integrating over velocity space. The result is a hierarchy of coupled differential equations—the transport or fluid equations—which describe the spatio-temporal variation of the moments of the velocity distribution functions of the electrons and ions species. In doing so the detailed features of the microscopic VDF are lost (i.e., the existence of non-Maxwellian features in the energy spectrum of particles or asymmetries in their pitch angle distributions). Indeed, there is an infinite variety of VDFs, which share the same values for their lowest order moments (Schunk and Watkins 1979).

The hydrodynamical transport models of varying degrees of sophistication which have been promoted for decades to describe ionospheric and interplanetary space plasmas appear to be easier to integrate than kinetic equations in the case of time dependent situations. By combining the moment equations for the electrons with those for the ions (often all species are assumed to have a common bulk velocity, $\boldsymbol{v} = \boldsymbol{E} \times \boldsymbol{B}/B^2$ as well as the same temperatures), one gets the standard MHD approximation of classical physics.

Furthermore, in the restrictive case of ideal MHD, it is postulated that $\boldsymbol{E} \cdot \boldsymbol{B} = 0$, i.e., that the electric field $\boldsymbol{E}$ has no component parallel to the magnetic field $\boldsymbol{B}$. To justify this ideal MHD approximation, the electrical conductivity of (almost) collisionless space plasmas should be (almost) infinitely large, so that, according to Ohm's law any small parallel electric field would imply an almost infinitely large value for the field-aligned current (i.e., Birkeland currents). This is based on the postulate that the traditional form of Ohm's law remains applicable even in collisionless plasmas. However, this is not quite the case in nearly collisionless magnetospheric plasma, where a generalized form of Ohm's law has to be used instead of its simplified form, which is only applicable in highly collision dominated plasmas. Wave-particle interactions produce a linear, ohmic type of anomalous resistivity, but

convincing experimental evidence remains to be found to assess their importance in scattering and heating the bulk of cold plasma in the ionosphere and plasmasphere.

Ideal MHD transport equations have been applied with mixed success in the study of a wide variety of space plasma physics problems. The more comprehensive multi-fluid moment equations and hydrodynamic transport equations consist of coupled sets of continuity, momentum and energy equations for each individual particle species separately. Reviews of different approximations for the multi-fluids transport equations used to study the solar wind, the polar wind and the refilling of empty plasmaspheric flux tubes can be found in the papers by Schunk (1988), Gombosi and Rasmussen (1991), Singh and Horwitz (1992) and Guiter et al. (1995).

Comparisons of transport models and kinetic or hybrid (semi-kinetic) models can be found in Holzer et al. (1971), Schunk and Watkins (1981), Demars and Schunk (1986) and Demars and Schunk (1991). These two complementary approaches were also used to model the solar wind and the polar wind (Lemaire and Echim 2008). In the following, we briefly overview how these models have been applied in the past to describe the refilling of plasmaspheric flux tubes that have been emptied or almost during a substorm (Horwitz and Singh 1991; Krall et al. 2008, and references therein).

### 4.1 Time Dependent Models for Field-Aligned Plasma Density Distribution

Time dependent and three dimensional models of the middle and high latitude ionosphere have been available for several decades (Schunk 1988). The more recent of these models take into account photochemistry, recombination processes and production of various ions due to reactions with the neutral atmosphere. They are based on the transport equations for mass, momentum and energy for the various ions (Singh et al. 1986; Rasmussen and Schunk 1988). Ion flows across magnetic field lines have been taken into account in several time dependent models and simulations for various given convection electric field models. The effects of counter-streaming of $H^+$ and $He^+$ along plasmaspheric tubes have been comprehensively studied by Rasmussen and Schunk (1988) and Krall et al. (2008).

The main constituents of the neutral atmosphere at great heights are helium and hydrogen. Hydrogen ions are formed by the charge exchange reaction $O^+ + H \Leftrightarrow O + H^+$. This reaction is accidentally resonant and proceeds at almost the same rate in both directions. Therefore, the main sink for $H^+$ ions is the reverse reaction. Throughout the F-region, there are sufficient collisions to maintain $H^+$ in chemical equilibrium. However, in the topside ionosphere where the $O^+$ density falls below approximately $5 \times 10^4\ \mathrm{cm}^{-3}$, $H^+$ ions are able to diffuse along magnetic field lines. The direction of the $H^+$ diffusion velocity depends mainly on the relative densities of the species involved in the charge exchange reaction.

When the plasmasphere is depleted, more $H^+$ ions are produced by the forward reaction than are removed by the reverse process. This leads to a net upward flow of $H^+$ into the plasmasphere. However, there is a limit to the rate at which the plasmasphere can be replenished by the upward $H^+$ flux (Hanson and Patterson 1963). Geisler (1967) indicated that the most important factor limiting the magnitude of the upward $H^+$ flux is the neutral hydrogen density.

### 4.2 Time Dependent Refilling Model

The first time dependent plasmaspheric flux tube refilling model was proposed by Banks et al. (1971). It is known as the "two-stage refilling scenario" and has been expanded until in the late 1980s within the framework of various hydrodynamical approximations (Singh

1988). According to this scenario a polar wind like supersonic flow is driven out of the ionosphere by a large pressure gradient parallel to the magnetic field lines. These flows from the conjugate hemispheres collide at the equator. A pair of shocks is formed as a consequence of this collision in the equatorial region. The shocks propagate downward, one in each hemisphere. Between the shocks the plasma is dense and warm, while below the shocks the upward flows are supersonic. This corresponds to the well-known scenario of refilling from "top to bottom".

Furthermore, it was proposed that when the shocks reach the ionosphere, a second phase of refilling process should follow, with upward subsonic flows lasting for several days. In such single-stream hydrodynamic models, the flux tube refills from top to bottom. So far, however, there is no evidence in CLUSTER and IMAGE observations for this early refilling scenario. As soon as the density becomes high enough, Coulomb collisions are an important factor in thermalizing the plasma flow (Grebowsky 1972; Khazanov et al. 1984; Guiter and Gombosi 1990).

Lemaire (2001) has suggested that the deceleration and deflection of the upwelling plasma streams generate intense electrostatic emissions detected outside the plasmasphere, where geomagnetic flux tubes are refilling. Strong electrostatic emissions sharply confined between $\pm 2^{\circ}$ of latitude (very close to the geomagnetic equatorial surface) have been observed by WHISPER onboard CLUSTER, on partially depleted flux tubes beyond the plasmapause (El-Lemdani Mazouz et al. 2006). Similarly confined intense electrostatic noise had already been observed in the equatorial region with wave antennae on earlier magnetospheric missions.

No definite picture has yet emerged describing how, when and where the downward or upward propagating shocks would form, if they do so at all. From IMAGE RPI measurements there does not seem to be any evidence for such propagating shocks in the observed field aligned plasma distribution. This supports then the kinetic refilling scenarios of Lemaire (1989), as well as those of obtained with the Monte Carlo simulations described above (Lin et al. 1992; Wilson et al. 1992). No such shocks are formed in the refilling plasmaspheric flux tubes. Moreover, using CLUSTER data Darrouzet et al. (2006) found that there is no evidence for sharp density gradients along field lines, such as would be expected in refilling shock fronts propagating along field lines.

Liemohn et al. (1999) have developed a time-dependent kinetic model to investigate the effects of self-consistency and hot plasma influences on plasmaspheric refilling. The model employs a direct solution of the kinetic equation with a Fokker-Planck Coulomb collision operator to obtain the phase space distribution function of the thermal protons along a field line. Investigations of the effects of anisotropic hot plasma populations on the refilling rates shows that, after a slight initial decrease in equatorial density from clearing out the initial distribution, there is a 10 to 30% increase after 4 hours due to these populations. This increase is due primarily to a slowing of the refilling streams near the equator from the reversed electric field.

### 4.3 Other Models of the Plasmasphere

Finally, let us mention some other plasmaspheric models. An excellent review of the major advances in plasmaspheric research made just before the launch of CLUSTER and IMAGE spacecraft was presented in Ganguli et al. (2000).

The FLIP (Field Line Interhemispheric Plasma) model (Richards and Torr 1986) is a fluid model that solves the equations of continuity, momentum and energy conservation of the particles in both hemispheres. It has been used to analyze the RPI IMAGE observations

of electron density along field lines (Tu et al. 2003). The calculated densities in the regions far from the equator were much lower than observed values, while good agreement was obtained in the equator.

Another physics-based model of the plasmasphere has been developed by Webb and Essex (2004). Their three-dimensional Global Plasmasphere Ionosphere Density (GPID) model uses a dynamic diffusive equilibrium approach within each magnetic flux tube. This theoretical model constitutes an improvement compared to the purely empirical models of the plasmasphere.

A Multi Species Kinetic Plasmaspheric Model (MSKPM) has been developed by Reynolds et al. (2001). This kinetic model is coupled to a parameterization of a fluid model of the ionosphere at the ion exobase. The hydrogen ion and helium ion density in the equatorial plane are found to exhibit local-time variations that are sensitive to the details of the exobase conditions and the diurnal convection. The theoretical predictions of the kinetic model were also compared with the quiet-time structure of the plasmaspheric density investigated using observations of the LANL geosynchronous satellites (Reynolds et al. 2003).

Note also Maruyama et al. (2005) who have modeled the response to a geomagnetic storm using the Rice Convection Model (RCM) and the Coupled Thermosphere-Ionosphere-Plasmasphere-electrodynamics (CTIPe) model. CTIPe is a global, three-dimensional, time-dependent, non-linear code including three physical components: a code for the neutral thermosphere, an ionospheric convection model and plasmaspheric model (Milward et al. 1996). Maruyama et al. (2005) show that during daytime, and at the early stage of the storm, the penetration electric field is dominant, while at night, the penetration and disturbance dynamo effects are comparable.

SAMI2 is Another low-latitude Model of the Ionosphere developed at the Naval Research Laboratory (Huba et al. 2000). SAMI2 treats the dynamic plasma and chemical evolution of seven ion species in the altitude range of 100 km to several thousand kilometers. The ion continuity and momentum equations are solved for all seven species. It models the plasma along the Earth's dipole field from hemisphere to hemisphere, includes the $\boldsymbol{E} \times \boldsymbol{B}$ drift of a flux tube (both in altitude and in longitude), and includes ion inertia in the ion momentum equation for motion along the dipole field line.

A physics-based data assimilation model of the ionosphere and neutral atmosphere called the Global Assimilation of Ionospheric Measurements (GAIM) has been developed by Schunk et al. (2004). GAIM uses a physics-based ionosphere-plasmasphere model and a Kalman filter for assimilating near real-time measurements including in situ density measurements from satellites, ionosonde electron density profiles, occultation data, measurements of the total electron contents (TECs) by Global Positioning System (GPS) satellites, two-dimensional ionospheric density distributions from tomography chains, and line-of-sight UV emissions from selected satellites.

## 5 Conclusions

The plasmasphere is an active part of a coupled global system. In the decades since the discovery of the plasmasphere and prior to the IMAGE and CLUSTER mission, the prevailing view of the plasmasphere was of a placid, passive component in the larger magnetospheric system. One of the main insights gleaned from plasmaspheric modeling in the era of global imaging observations is that, contrary to the previously prevailing view, the plasmasphere plays a very active role in the dynamics of the rest of the magnetosphere.

The plasmasphere-magnetosphere interaction is two-way. Convection terms, such as shielding and SAPS, produced by the interactions among non-plasmaspheric populations,

such as the ring current and ionosphere, certainly exert a profound and controlling influence upon the dynamics of the plasmasphere. In turn, plasmaspheric dynamics then influence the dynamics of other populations, such as the ring current and radiation belts.

This system-level perspective extends to other populations as well, as illustrated by the need for a self-consistent determination of the inner magnetospheric electric field produced by ring-current-ionosphere coupling. In the post-IMAGE era, we have a deeper understanding of how all the various components of the magnetosphere mesh together into a single system of intimately-coupled plasmas and fields. Moreover, the four CLUSTER satellites provided for the first time highly precise and three-dimensional measurements allowing to better understand the physical mechanisms implicated in the dynamics of the plasmasphere, the formation of the plasmapause and the development of plumes.

**Acknowledgements** V. Pierrard and J. Lemaire acknowledge the support by the Belgian Federal Science Policy Office (BELSPO) through the ESA/PRODEX CLUSTER project (contract 13127/98/NL/VJ (IC)). Work at Los Alamos was conducted under the auspices of the U. S. Department of Energy, with partial support from the NASA LWS and GI programs, and from a Los Alamos National Laboratory Directed Research and Development grant. This paper is an outcome of the workshop "The Earth's plasmasphere: A CLUSTER, IMAGE, and modeling perspective", organized by the Belgian Institute for Space Aeronomy in Brussels in September 2007.

## References

M.L. Adrian, D.L. Gallagher, L.A. Avanov, IMAGE EUV observation of radially bifurcated plasmaspheric features: First observations of a possible standing ULF waveform in the inner magnetosphere. J. Geophys. Res. **109**, A01203 (2004)

B.J. Anderson, R.E. Erlandson, L.J. Zanetti, A statistical study of pc 1–2 magnetic pulsations in the equatorial magnetosphere 1. Equatorial occurrence distributions. J. Geophys. Res. **97**(A3), 3075–3088 (1992)

P.C. Anderson, D.L. Carpenter, K. Tsuruda, T. Mukai, F.J. Rich, Multisatellite observations of rapid subauroral ion drifts (SAID). J. Geophys. Res. **106**(A12), 29585–29599 (2001)

N. André, Ondes et instabilités basse-fréquence dans un plasma gyrotrope. Application à l'instabilité d'interchange dans les magnétosphères des planètes géantes. PhD thesis, Université Paul Sabatier, Toulouse, France, 2003

N. André, K.M. Ferrière, Low-frequency waves and instabilities in stratified, gyrotropic, multicomponent plasmas: Theory and application to plasma transport in the Io torus. J. Geophys. Res. **109**, A12225 (2004)

N. André, J.F. Lemaire, Convective instabilities in the plasmasphere. J. Atmos. Sol.-Terr. Phys. **68**(2), 213–227 (2006)

G.J. Bailey, N. Balan, Y.Z. Su, The Sheffield University plasmasphere ionosphere model—A review. J. Atmos. Sol-Terr. Phys. **59**(13), 1541–1552 (1997)

P.M. Banks, A.F. Nagy, W.I. Axford, Dynamical behavior of thermal protons in mid-latitude ionosphere and magnetosphere. Planet. Space Sci. **19**(9), 1053–1067 (1971)

A.R. Barakat, I.A. Barghouthi, The effect of wave-particle interactions on the polar wind $O^+$. Geophys. Res. Lett. **21**(21), 2279–2282 (1994)

A.R. Barakat, R.W. Schunk, I.A. Barghouti, J. Lemaire, Monte-Carlo study of the transition from collision-dominated to collisionless polar wind flow, in *Physics of Space Plasmas*, ed. by T. Chang, G.B. Crew, J.R. Jaspers (Scientific Publisher, Cambridge, 1990), pp. 431–437

A.R. Barakat, I.A. Barghouthi, R.W. Schunk, Double-hump $H^+$ velocity distribution in the polar wind. Geophys. Res. Lett. **22**(14), 1857–1860 (1995)

I.A. Barghouthi, A.R. Barakat, R.W. Schunk, Monte Carlo study of the transition region in the polar wind: An improved collision model. J. Geophys. Res. **98**(A10), 17583–17591 (1993)

I.A. Barghouthi, V. Pierrard, A.R. Barakat, J. Lemaire, A Monte Carlo simulation of the $H^+$ polar wind: Effect of velocity distributions with Kappa suprathermal tails. Astrophys. Space Sci. **277**(3), 427–436 (2001)

I.A. Barghouthi, N.M. Doudin, A.A. Saleh, V. Pierrard, High-altitude and high-latitude $O^+$ and $H^+$ outflows: the effect of finite electromagnetic turbulence wavelength. Ann. Geophys. **25**(10), 2195–2202 (2007)

I.A. Barghouthi, N.M. Doudin, A.A. Saleh, V. Pierrard, The effect of altitude- and velocity-dependent wave–particle interactions on the $H^+$ and $O^+$ outflows in the auroral region. J. Atmos. Sol.-Terr. Phys. **70**(8–9), 1159–1169 (2008)

S.J. Bauer, On the structure of the topside ionosphere. J. Atmos. Sci. **19**(3), 276–278 (1962)

V.V. Bezrukikh, G.A. Kotova, L.A. Lezhen, J. Lemaire, V. Pierrard, Yu.I. Venediktov, Dynamics of temperature and density of cold protons of the Earth's plasmasphere measured by the Auroral Probe/Alpha-3 experiment data during geomagnetic disturbances. Cosm. Res. **41**(4), 392–402 (2003)

D. Bilitza, International reference ionosphere: Recent developments. Radio Sci. **21**(3), 343–346 (1986)

J.E. Borovsky, M. Hesse, The reconnection of magnetic fields between plasmas with different densities: Scaling relations. Phys. Plasmas **14**(10), 102309 (2007)

J.L. Burch, IMAGE mission overview. Space Sci. Rev. **91**(1–2), 1–14 (2000)

J.L. Burch, J. Goldstein, B.R. Sandel, Cause of plasmasphere corotation lag. Geophys. Res. Lett. **31**, L02502 (2004)

J.L. Burch, W.S. Lewis, T.J. Immel, P.C. Anderson, H.U. Frey, S.A. Fuselier, J.C. Gérard, S.B. Mende, D.G. Mitchell, M.F. Thomsen, Interplanetary magnetic field control of afternoon-sector detached proton auroral arcs. J. Geophys. Res. **107**(A9), 1251 (2005)

W.I. Burke, N.C. Maynard, M.P. Hagan, R.A. Wolf, G.R. Wilson, L.C. Gentile, M.S. Gussenhoven, C.Y. Huang, T.W. Garner, F.J. Rich, Electrodynamics of the inner magnetosphere observed in the dusk sector by CRRES and DMSP during the magnetic storm of June 4–6, 1991. J. Geophys. Res. **103**(A12), 29399–29418 (1998)

D.L. Carpenter, Whistler studies of the plasmapause in the magnetosphere, 1. Temporal variations in the position of the knee and some evidence on plasma motions near the knee. J. Geophys. Res. **71**(3), 693–709 (1966)

D.L. Carpenter, R.R. Anderson, An ISEE/whistler model of equatorial electron density in the magnetosphere. J. Geophys. Res. **97**(A2), 1097–1108 (1992)

D.L. Carpenter, J. Lemaire, The plasmasphere boundary layer. Ann. Geophys. **22**(12), 4291–4298 (2004)

D.L. Carpenter, B.L. Giles, C.R. Chappell, P.M.E. Décréau, R.R. Anderson, A.M. Persoon, A.J. Smith, Y. Corcuff, P. Canu, Plasmasphere dynamics in the duskside bulge region: A new look at an old topic. J. Geophys. Res. **98**(A11), 19243–19271 (1993)

C.R. Chappell, Recent satellite measurements of the morphology and dynamics of the plasmasphere. Rev. Geophys. Space Phys. **10**(4), 951–979 (1972)

C.R. Chappell, Detached plasma regions in the magnetosphere. J. Geophys. Res. **79**(13), 1861–1870 (1974)

C.R. Chappell, T.E. Moore, J.H. Waite Jr., The ionosphere as a fully adequate source of plasma for the Earth's magnetosphere. J. Geophys. Res. **92**(A6), 5896–5910 (1987)

S.H. Chen, T.E. Moore, Magnetospheric convection and thermal ions in the dayside outer magnetosphere. J. Geophys. Res. **111**, A03215 (2006)

A.J. Chen, R.A. Wolf, Effects on the plasmasphere of a time-varying convection electric field. Planet. Space Sci. **20**(4), 483–509 (1972)

A.J. Chen, J.M. Grebowsky, H.A. Taylor Jr., Dynamics of mid-latitude light ion trough and plasma tails. J. Geophys. Res. **80**(7), 968–976 (1975)

A.F. Cheng, Magnetospheric interchange instability. J. Geophys. Res. **90**(A10), 9900–9904 (1989)

R.H. Comfort, Plasmasphere thermal structure as measured by ISEE-1 and DE-1. Adv. Space Res. **6**(3), 31–40 (1986)

R.H. Comfort, Thermal structure of the plasmasphere. Adv. Space Res. **17**(10), 175–184 (1996)

J.M. Cornwall, F.V. Coroniti, R.M. Thorne, Turbulent loss of ring current protons. J. Geophys. Res. **75**(25), 4699–4709 (1970)

I. Dandouras, Detection of plasmaspheric wind by analysis of ion measurements obtained onboard the Cluster spacecraft. Geophys. Res. Abstr. **10**, 5360 (2008)

I. Dandouras, V. Pierrard, J. Goldstein, C. Vallat, G.K. Parks, H. Rème, C. Gouillart, F. Sevestre, M. McCarthy, L.M. Kistler, B. Klecker, A. Korth, M.B. Bavassano-Cattaneo, P. Escoubet, A. Masson, Multipoint observations of ionic structures in the plasmasphere by CLUSTER-CIS and comparisons with IMAGE-EUV observations and with model simulations, in *Inner Magnetosphere Interactions: New Perspectives from Imaging*, ed. by J.L. Burch, M. Schulz, H. Spence. Geophysical Monograph Series, vol. 159 (American Geophysical Union, Washington, 2005), pp. 23–53

F. Darrouzet, Etude de la magnétosphère terrestre par l'analyse multipoint des données de la mission CLUSTER. Contributions à la caractérisation des frontières et de la magnétosphère interne. PhD thesis, University of Orléans, France, 2006. http://www.aeronomie.be/plasmasphere/pdf/Darrouzet_PhDThesis_UniversityOrleans_20060607.pdf

F. Darrouzet, J. De Keyser, P.M.E. Décréau, J.F. Lemaire, M.W. Dunlop, Spatial gradients in the plasmasphere from Cluster. Geophys. Res. Lett. **33**, L08105 (2006)

F. Darrouzet, D.L. Gallagher, N. André, D.L. Carpenter, I. Dandouras, P.M.E. Décréau, J. De Keyser, R.E. Denton, J.C. Foster, J. Goldstein, M.B. Moldwin, B.W. Reinisch, B.R. Sandel, J. Tu, Plasmaspheric density structures and dynamics: Properties observed by the CLUSTER and IMAGE missions. Space Sci. Rev. (2008, this issue)

J. De Keyser, D.L. Carpenter, F. Darrouzet, D.L. Gallagher, J. Tu, CLUSTER and IMAGE: New ways to study the Earth's plasmasphere. Space Sci. Rev. (2008, this issue)

P.M.E. Décréau, P. Fergeau, V. Krasnosels'kikh, E. Le Guirriec, M. Lévêque, P. Martin, O. Randriamboarison, J.L. Rauch, F.X. Sené, H.C. Séran, J.G. Trotignon, P. Canu, N. Cornilleau, H. de Féraudy, H. Alleyne, K. Yearby, P.B. Mögensen, G. Gustafsson, M. André, D.A. Gurnett, F. Darrouzet, J. Lemaire, C.C. Harvey, P. Travnicek, Whisper experimenters, Early results from the Whisper instrument on Cluster: An overview. Ann. Geophys. **19**(10–12), 1241–1258 (2001)

H.G. Demars, R.W. Schunk, Solutions to bi-Maxwellian transport equations for SAR-arc conditions. Planet. Space Sci. **34**(12), 1335–1348 (1986)

H.G. Demars, R.W. Schunk, Comparison of semi-kinetic and generalized transport models of the polar wind. Geophys. Res. Lett. **18**(4), 713–716 (1991)

M. Echim, J. Lemaire, Two-dimensional Vlasov solution for a collisionless plasma jet across transverse magnetic field lines with a sheared bulk velocity. Phys. Rev. E **72**(3), 036405 (2005)

F. El-Lemdani Mazouz, S. Grimald, J.L. Rauch, P.M.E. Décréau, G. Bozan, G. Le Rouzic, X. Suraud, X. Vallières, J.G. Trotignon, P. Canu, F. Darrouzet, S. Boardsen, Electrostatic and electromagnetic emissions near the plasmasphere. A case event: 27 May 2003, in *Proceedings of the Cluster and Double Star Symposium, 5th Anniversary of Cluster in Space* **ESA SP-598** (2006)

R.C. Elphic, L.A. Weiss, M.F. Thomsen, D.J. McComas, M.B. Moldwin, Evolution of plasmaspheric ions at geosynchronous orbit during times of high geomagnetic activity. Geophys. Res. Lett. **23**(16), 2189–2192 (1996)

M.J. Engebretson, W.J. Hughes, J.L. Alford, E. Zesta, L.J. Cahill Jr., R.L. Arnoldy, G.D. Reeves, Magnetometer array for cusp and cleft studies observations of the spatial extent of broadband ULF magnetic pulsations at cusp/cleft latitudes. J. Geophys. Res. **100**(A10), 19371–19386 (1995)

A. Eviatar, A.M. Lenchek, S.F. Singer, Distribution of density in an ion-exosphere of a nonrotating planet. Phys. Fluids **7**(11), 1775–1779 (1964)

H.J. Fahr, B. Shizgal, Modern exospheric theories and their observational relevance. Rev. Geophys. Space Phys. **21**(1), 75–124 (1983)

C.J. Farrugia, M.P. Freeman, S.W.H. Cowley, D.J. Southwood, M. Lockwood, A. Etemadi, Pressure-driven magnetopause motions and attendant response on the ground. Planet. Space Sci. **37**(5), 589–607 (1989)

K.M. Ferrière, N. André, A mixed magnetohydrodynamic-kinetic theory of low-frequency waves and instabilities in stratified, gyrotropic, two-component plasmas. J. Geophys. Res. **108**(A7), 1308 (2003)

K.M. Ferrière, C. Zimmer, M. Blanc, Magnetohydrodynamic waves and gravitational/centrifugal instability in rotating magnetospheres. J. Geophys. Res. **104**(A8), 17335–17356 (1999)

J.C. Foster, W.J. Burke, SAPS: A new categorization for sub-auroral electric fields. Eos Trans. AGU **83**(36), 393 (2002)

J.C. Foster, A.J. Coster, P.J. Erickson, F.J. Rich, B.R. Sandel, Stormtime observations of the flux of plasmaspheric ions to the dayside cusp/magnetopause. Geophys. Res. Lett. **31**, L08809 (2004)

D.L. Gallagher, M.L. Adrian, M.W. Liemohn, Origin and evolution of deep plasmaspheric notches. J. Geophys. Res. **110**, A09201 (2005)

Y.I. Galperin, V.N. Ponomarev, A.G. Zosimova, Plasma convection in the polar ionosphere. Ann. Geophys. **30**(1), 1–7 (1974)

G. Ganguli, M.A. Reynolds, M.W. Liemohn, The plasmasphere and advances in plasmaspheric research. J. Atmos. Sol.-Terr. Phys. **62**(17–18), 1647–1657 (2000)

S.P. Gary, M.F. Thomsen, L. Yin, D. Winske, Electromagnetic proton cyclotron instability: Interactions with magnetospheric protons. J. Geophys. Res. **100**(A11), 21961–21972 (1995)

J.E. Geisler, On the limiting daytime flux of ionization into the protonosphere. J. Geophys. Res. **72**(1), 81–85 (1967)

T. Gold, Motions in the magnetosphere of the Earth. J. Geophys. Res. **64**(9), 1219–1224 (1959)

J. Goldstein, B.R. Sandel, The global pattern of evolution of plasmaspheric drainage plumes, in *Inner Magnetosphere Interactions: New Perspectives from Imaging*, ed. by J.L. Burch, M. Schulz, H. Spence. Geophysical Monograph Series, vol. 159 (American Geophysical Union, Washington, 2005), pp. 1–22

J. Goldstein, R.W. Spiro, P.H. Reiff, R.A. Wolf, B.R. Sandel, J.W. Freeman, R.L. Lambour, IMF-driven overshielding electric field and the origin of the plasmaspheric shoulder of May 24, 2000. Geophys. Res. Lett. **29**(16), 1819 (2002)

J. Goldstein, B.R. Sandel, M.R. Hairston, P.H. Reiff, Control of plasmaspheric dynamics by both convection and sub-auroral polarization stream. Geophys. Res. Lett. **30**(24), 2243 (2003a)

J. Goldstein, M. Spasojević, P.H. Reiff, B.R. Sandel, W.T. Forrester, D.L. Gallagher, B.W. Reinisch, Identifying the plasmapause in IMAGE EUV data using IMAGE RPI in situ steep density gradients. J. Geophys. Res. **108**(A4), 1147 (2003b)
J. Goldstein, B.R. Sandel, W.T. Forrester, P.H. Reiff, IMF-driven plasmasphere erosion of 10 July 2000. Geophys. Res. Lett. **30**(3), 1146 (2003c)
J. Goldstein, R.W. Spiro, B.R. Sandel, R.A. Wolf, S.Y. Su, P.H. Reiff, Overshielding event of 28–29 July 2000. Geophys. Res. Lett. **30**(8), 1421 (2003d)
J. Goldstein, B.R. Sandel, M.F. Thomsen, M. Spasojević, P.H. Reiff, Simultaneous remote sensing and in situ observations of plasmaspheric drainage plumes. J. Geophys. Res. **109**, A03202 (2004)
J. Goldstein, J.L. Burch, B.R. Sandel, Magnetospheric model of subauroral polarization stream. J. Geophys. Res. **110**, A09222 (2005a)
J. Goldstein, B.R. Sandel, W.T. Forrester, M.F. Thomsen, M.R. Hairston, Global plasmasphere evolution 22–23 April 2001. J. Geophys. Res. **110**, A12218 (2005b)
T.I. Gombosi, C.E. Rasmussen, Transport of gyration-dominated space plasmas of thermal origin 1. Generalized transport equations. J. Geophys. Res. **96**(A5), 7759–7778 (1991)
J.M. Grebowsky, Model study of plasmapause motion. J. Geophys. Res. **75**(22), 4329–4333 (1970)
J.M. Grebowsky, Model development of supersonic trough wind with shocks. Planet. Space Sci. **20**(11), 1923–1934 (1972)
J.M. Grebowsky, A.J. Chen, Effects on the plasmasphere of irregular electric fields. Planet. Space Sci. **24**(7), 689–696 (1976)
K.I. Gringauz, V.V. Bezrukikh, V.D. Ozerov, R.E. Rybchinskii, The study of the interplanetary ionized gas, high-energy electrons and corpuscular radiation of the Sun, employing three-electrode charged particle traps on the second Soviet space rocket. Sov. Phys. Dokl. **5**, 361–364 (1960). Published again in (1962) in Planet. Space Sci. **9**, 103–107
S.M. Guiter, T.I. Gombosi, The role of high-speed plasma flows in plasmaspheric refilling. J. Geophys. Res. **95**(A7), 10427–10440 (1990)
S.M. Guiter, T.I. Gombosi, C.E. Rasmussen, Two-stream modeling of plasmaspheric refilling. J. Geophys. Res. **100**(A6), 9519–9526 (1995)
M.S. Gussenhoven, D.A. Hardy, W.J. Burke, DMSP/F2 electron observations of equatorward auroral boundaries and their relationship to magnetospheric electric fields. J. Geophys. Res. **86**(A2), 768–778 (1981)
W.B. Hanson, T.N.L. Patterson, Diurnal variation of the hydrogen concentration in the exosphere. Planet. Space Sci. **11**(9), 1035–1052 (1963)
A.E. Hedin, MSIS-86 thermospheric model. J. Geophys. Res. **92**(A5), 4649–4662 (1987)
T.E. Holzer, J.A. Fedder, P.M. Banks, A comparison of kinetic and hydrodynamic models of an expanding ion-exosphere. J. Geophys. Res. **76**(A10), 2453–2468 (1971)
J.L. Horwitz, N. Singh, Refilling of the Earth's plasmasphere. Eos Trans. AGU **72**(37), 399–402 (1991)
J.L. Horwitz, C.R. Baugher, C.R. Chappell, E.G. Shelley, D.T. Young, R.R. Anderson, ISEE 1 observations of thermal plasma in the vicinity of the plasmasphere during periods of quieting magnetic activity. J. Geophys. Res. **86**(A12), 9989–10001 (1981)
J.D. Huba, G. Joyce, J.A. Fedder, Sami2 is another model of the ionosphere (SAMI2): A new low-latitude ionosphere model. J. Geophys. Res. **105**(A10), 23035–23053 (2000)
T. Iijima, T.A. Potemra, The amplitude distribution of field-aligned currents at northern high latitudes observed by Triad. J. Geophys. Res. **81**(13), 2165–2174 (1976)
T.J. Immel, S.B. Mende, H.U. Frey, L.M. Peticolas, C.W. Carlson, J.C. Gérard, B. Hubert, S.A. Fuselier, J.L. Burch, Precipitation of auroral protons in detached arcs. Geophys. Res. Lett. **29**(11), 1519 (2002)
R.K. Jaggi, R.A. Wolf, Self-consistent calculation of the motion of a sheet of ions in the magnetosphere. J. Geophys. Res. **78**(16), 2852–2866 (1973)
V.K. Jordanova, L.M. Kistler, J.U. Kozyra, G.V. Khazanov, A.F. Nagy, Collisional losses of ring current ions. J. Geophys. Res. **101**(A1), 111–126 (1996a)
V.K. Jordanova, J.U. Kozyra, A.F. Nagy, Effects of heavy ions on the quasi-linear diffusion coefficients from resonant interactions with electromagnetic ion cyclotron waves. J. Geophys. Res. **101**(A9), 19771–19778 (1996b)
V.K. Jordanova, J.U. Kozyra, A.F. Nagy, G.V. Khazanov, Kinetic model of the ring current-atmosphere interactions. J. Geophys. Res. **102**(A7), 14279–14291 (1997)
V.K. Jordanova, Y.S. Miyoshi, S. Zaharia, M.F. Thomsen, G.D. Reeves, D.S. Evans, C.G. Mouikis, J.F. Fennell, Kinetic simulations of ring current evolution during the Geospace Environment Modeling challenge events. J. Geophys. Res. **111**, A11S10 (2006)
V.K. Jordanova, M. Spasojevic, M.F. Thomsen, Modeling the electromagnetic ion cyclotron wave-induced formation of detached subauroral proton arcs. J. Geophys. Res. **112**, A08209 (2007)
G.V. Khazanov, M.A. Koyen, Y.V. Konikov, I.M. Sidorov, Simulation of ionosphere-plasmasphere coupling taking into account ion inertia and temperature anisotropy. Planet. Space Sci. **32**(5), 585–598 (1984)

G.A. Kotova, The Earth's plasmasphere: state of studies (a review). Geomagn. Aeron. **47**(4), 409–422 (2007)
G.A. Kotova, V.V. Bezrukikh, M.I. Verigin, L.A. Lezhen, Temperature and density variations in the dusk and dawn plasmasphere as observed by Interball Tail in 1999–2000. Adv. Space Res. **30**(7), 1831–1834 (2002)
J. Krall, J.D. Huba, J.A. Fedder, Simulation of field-aligned $H^+$ and $He^+$ dynamics during late-stage plasmasphere refilling. Ann. Geophys. **26**(6), 1507–1516 (2008)
R.L. Lambour, L.A. Weiss, R.C. Elphic, M.F. Thomsen, Global modeling of the plasmasphere following storm sudden commencements. J. Geophys. Res. **102**(A11), 24351–24368 (1997)
M.J. LeDocq, D.A. Gurnett, R.R. Anderson, Electron number density fluctuations near the plasmapause observed by the CRRES spacecraft. J. Geophys. Res. **99**(A12), 23661–23671 (1994)
J.F. Lemaire, The "Roche-limit" of ionospheric plasma and the formation of the plasmapause. Planet. Space Sci. **22**(5), 757–766 (1974)
J. Lemaire, Rotating ion-exospheres. Planet. Space Sci. **24**(10), 975–985 (1976)
J.F. Lemaire, *Frontiers of the Plasmasphere*. Aeronomica Acta **A298** (1985)
J.F. Lemaire, Plasma distribution models in a rotating magnetic dipole and refilling plasmaspheric flux tubes. Phys. Fluids B **1**(7), 1519–1525 (1989)
J.F. Lemaire, Hydrostatic equilibrium and convective stability in the plasmasphere. J. Atmos. Sol.-Terr. Phys. **61**(11), 867–878 (1999)
J.F. Lemaire, The formation plasmaspheric tails. Phys. Chem. Earth (C) **25**, 9–17 (2000)
J.F. Lemaire, The formation of the light-ion-trough and peeling off the plasmasphere. J. Atmos. Sol.-Terr. Phys. **63**(11), 1285–1291 (2001)
J.F. Lemaire, M. Echim, Kinetic and hydrodynamic models of the solar wind and polar wind. Eos Trans. AGU **89**(9), 86 (2008)
J.F. Lemaire, K.I. Gringauz, *The Earth's Plasmasphere* (Cambridge University Press, New York, 1998), p. 372
J. Lemaire, V. Pierrard, Kinetic models of solar and polar winds. Astrophys. Space Sci. **277**(1–2), 169–180 (2001)
J.F. Lemaire, V. Pierrard, Comparison between two theoretical mechanisms for the formation of the plasmapause and relevant observations. Geomagn. Aeron. **48**(5), 553–570 (2008)
J.F. Lemaire, R.W. Schunk, Plasmaspheric wind. J. Atmos. Terr. Phys. **54**(3–4), 467–477 (1992)
J.F. Lemaire, R.W. Schunk, Plasmaspheric convection with non-closed streamlines. J. Atmos. Terr. Phys. **56**(12), 1629–1633 (1994)
Ø. Lie-Svendsen, M.H. Rees, An improved kinetic model for the polar outflow of a minor ion. J. Geophys. Res. **101**(A2), 2415–2433 (1996)
M.W. Liemohn, G.V. Khazanov, P.D. Craven, J.U. Kozyra, Nonlinear kinetic modeling of the early stage plasmaspheric refilling. J. Geophys. Res. **104**(A5), 10295–10306 (1999)
M.W. Liemohn, J.U. Kozyra, M.F. Thomsen, J.L. Roeder, G. Lu, J.E. Borovsky, T.E. Cayton, Dominant role of the asymmetric ring current in producing the stormtime Dst*. J. Geophys. Res. **106**(A6), 10883–10904 (2001)
M.W. Liemohn, A.J. Ridley, D.L. Gallagher, D.M. Ober, J.U. Kozyra, Dependence of plasmaspheric morphology on the electric field description during the recovery phase of the 17 April 2002 magnetic storm. J. Geophys. Res. **109**, A03209 (2004)
M.W. Liemohn, A.J. Ridley, P.C. Brandt, D.L. Gallagher, J.U. Kozyra, D.M. Ober, D.G. Mitchell, E.C. Roelof, R. DeMajistre, Parametric analysis of nightside conductance effects on inner magnetospheric dynamics for the 17 April 2002 storm. J. Geophys. Res. **110**, A12S22 (2005)
M.W. Liemohn, A.J. Ridley, J.U. Kozyra, D.L. Gallagher, M.F. Thomsen, M.G. Henderson, M.H. Denton, P.C. Brandt, J. Goldstein, Analyzing electric field morphology through data-model comparisons of the Geospace Environment Modeling Inner Magnetosphere/Storm Assessment Challenge events. J. Geophys. Res. **111**, A11S11 (2006)
J. Lin, J.L. Horwitz, G.R. Wilson, C.W. Ho, D.G. Brown, A semikinetic model for early stage plasmasphere refilling 2, Effects of wave-particle interactions. J. Geophys. Res. **97**(A2), 1121–1134 (1992)
N. Maruyama, A.D. Richmond, T.J. Fuller-Rowell, M.V. Codrescu, S. Sazykin, F.R. Toffoletto, R.W. Spiro, G.H. Millward, Interaction between direct penetration and disturbance dynamo electric fields in the storm-time equatorial ionosphere. Geophys. Res. Lett. **32**, L17105 (2005)
H. Matsui, T. Mukai, S. Ohtani, K. Hayashi, R.C. Elphic, M.F. Thomsen, H. Matsumoto, Cold dense plasma in the outer magnetosphere. J. Geophys. Res. **104**(A11), 25077–25095 (1999)
H. Matsui, M. Nakamura, T. Terasawa, Y. Izaki, T. Mukai, K. Tsuruda, H. Hayakawa, H. Matsumoto, Outflow of cold dense plasma associated with variation of convection in the outer magnetosphere. J. Atmos. Sol.-Terr. Phys. **62**(6), 521–526 (2000)
H. Matsui, J.M. Quinn, R.B. Torbert, V.K. Jordanova, W. Baumjohann, P.A. Puhl-Quinn, G. Paschmann, Electric field measurements in the inner magnetosphere by Cluster EDI. J. Geophys. Res. **108**(A9), 1352 (2003)

N.C. Maynard, A.J. Chen, Isolated cold plasma regions: Observations and their relation to possible production mechanisms. J. Geophys. Res. **80**(7), 1009–1013 (1975)
C.E. McIlwain, A $K_p$ dependent equatorial electric field model. Adv. Space Res. **6**(3), 187–197 (1986)
R.H. Miller, C.E. Rasmussen, T.I. Gombosi, G.V. Khazanov, D. Winske, Kinetic simulation of plasma flows in the inner magnetosphere. J. Geophys. Res. **98**(A11), 19301–19313 (1993)
G.H. Milward, R.J. Moffett, S. Quegan, T.J. Fuller-Rowell, A coupled thermosphere-ionosphere-plasmasphere model (CTIP), in *Solar Terrestrial Energy Program (STEP) Handbook on Ionospheric Models*, ed. by R.W. Schunk (Utah State University, Logan, 1996), pp. 239–279
D.B. Muldrew, F-layer ionization troughs deduced from Alouette data. J. Geophys. Res. **70**(11), 2635–2650 (1965)
W.A. Newcomb, Convective instability induced by gravity in a plasma with a frozen-in magnetic field. Phys. Fluids **4**(4), 391–396 (1961)
D.M. Ober, J.L. Horwitz, D.L. Gallagher, Formation of density troughs embedded in the outer plasmasphere by subauroral ion drift events. J. Geophys. Res. **102**(A7), 14595–14602 (1997)
G.K. Parks, *Physics of Space Plasmas: An Introduction* (Westview Press, Boulder, 2004), p. 597
V. Pierrard, New model of magnetospheric current-voltage relationship. J. Geophys. Res. **101**(A2), 2669–2675 (1996)
V. Pierrard, The dynamics of the plasmasphere, in *Space Science: New Research*, ed. by N.S. Maravell (Nova Science, New York, 2006), pp. 83–96
V. Pierrard, I.A. Barghouthi, Effects of wave-particle interactions on double-hump distributions of the $H^+$ polar wind. Astrophys. Space Sci. **302**(1–4), 35–41 (2006)
V. Pierrard, J. Cabrera, Comparisons between EUV/IMAGE observations and numerical simulations of the plasmapause formation. Ann. Geophys. **23**(7), 2635–2646 (2005)
V. Pierrard, J. Cabrera, Dynamical simulations of plasmapause deformations. Space Sci. Rev. **122**(1–4), 119–126 (2006)
V. Pierrard, J. Lemaire, Lorentzian ion exosphere model. J. Geophys. Res. **101**(A4), 7923–7934 (1996)
V. Pierrard, J. Lemaire, A collisional kinetic model of the polar wind. J. Geophys. Res. **103**(A6), 11701–11709 (1998)
V. Pierrard, J. Lemaire, Exospheric model of the plasmasphere. J. Atmos. Sol.-Terr. Phys. **63**(11), 1261–1265 (2001)
V. Pierrard, J.F. Lemaire, Development of shoulders and plumes in the frame of the interchange instability mechanism for plasmapause formation. Geophys. Res. Lett. **31**, L05809 (2004)
V. Pierrard, K. Stegen, A three-dimensional dynamic kinetic model of the plasmasphere. J. Geophys. Res. **113**, A10209 (2008)
V. Pierrard, M. Maksimovic, J. Lemaire, Electron velocity distribution functions from the solar wind to the corona. J. Geophys. Res. **104**(A8), 17021–17032 (1999)
V. Pierrard, G.V. Khazanov, J. Cabrera, J. Lemaire, Influence of the convection electric field models on predicted plasmapause positions during magnetic storms. J. Geophys. Res. **113**, A08212 (2008)
J.M. Quinn, G. Paschmann, N. Sckopke, V.K. Jordanova, H. Vaith, O.H. Bauer, W. Baumjohann, W. Fillius, G. Haerendel, S.S. Kerr, C.A. Kletzing, K. Lynch, C.E. McIlwain, R.B. Torbert, E.C. Whipple, EDI convection measurements at 5–6 $R_E$ in the post-midnight region. Ann. Geophys. **17**(12), 1503–1512 (1999)
C.E. Rasmussen, R.W. Schunk, Multistream hydrodynamic modeling of interhemispheric plasma flow. J. Geophys. Res. **93**(A12), 14557–14565 (1988)
C.E. Rasmussen, S.M. Guiter, S.G. Thomas, A two-dimensional model of the plasmasphere: refilling time constants. Planet. Space Sci. **41**(1), 35–43 (1993)
B.W. Reinisch, X. Huang, P. Song, J.L. Green, S.F. Fung, V.M. Vasyliunas, D.L. Gallagher, B.R. Sandel, Plasmaspheric mass loss and refilling as a result of a magnetic storm. J. Geophys. Res. **109**, A01202 (2004)
B.W. Reinisch, M.B. Moldwin, R.E. Denton, D.L. Gallagher, H. Matsui, V. Pierrard, J. Tu, Augmented empirical models of plasmaspheric density and electric field using IMAGE and CLUSTER data. Space Sci. Rev. (2008, this issue)
H. Rème, C. Aoustin, J.M. Bosqued, I. Dandouras, B. Lavraud, J.A. Sauvaud, A. Barthe, J. Bouyssou, Th. Camus, O. Coeur-Joly, A. Cros, J. Cuvilo, F. Ducay, Y. Garbarowitz, J.L. Médale, E. Penou, H. Perrier, D. Romefort, J. Rouzaud, C. Vallat, D. Alcaydé, C. Jacquey, C. Mazelle, C. d'Uston, E. Möbius, L.M. Kistler, K. Crocker, M. Granoff, C. Mouikis, M. Popecki, M. Vosbury, B. Klecker, D. Hovestadt, H. Kucharek, E. Kuenneth, G. Paschmann, M. Scholer, N. Sckopke, E. Seidenschwang, C.W. Carlson, D.W. Curtis, C. Ingraham, R.P. Lin, J.P. McFadden, G.K. Parks, T. Phan, V. Formisano, E. Amata, M.B. Bavassano-Cattaneo, P. Baldetti, R. Bruno, G. Chionchio, A. Di Lellis, M.F. Marcucci, G. Pallocchia, A. Korth, P.W. Daly, B. Graeve, H. Rosenbauer, V. Vasyliunas, M. McCarthy, M. Wilber, L. Eliasson, R. Lundin, S. Olsen, E.G. Shelley, S. Fuselier, A.G. Ghielmetti, W. Lennartsson, C.P. Escoubet,

H. Balsiger, R. Friedel, J.-B. Cao, R.A. Kovrazhkin, I. Papamastorakis, R. Pellat, J. Scudder, B. Sonnerup, First multi-spacecraft ion measurements in and near the Earth's magnetosphere with the identical Cluster Ion Spectrometry (CIS) experiment. Ann. Geophys. **19**(10–12), 1303–1354 (2001)

M.A. Reynolds, D.J. Meléndez-Alvira, G. Ganguli, Equatorial coupling between the plasmasphere and the topside ionosphere. J. Atmos. Sol.-Terr. Phys. **63**(11), 1267–1273 (2001)

M.A. Reynolds, G. Ganguli, Y.J. Su, M.F. Thomsen, The local-time variation of the quiet plasmasphere: geosynchronous observations and kinetic theory. Ann. Geophys. **21**(11), 2147–2154 (2003)

P.G. Richards, D.G. Torr, Thermal coupling of conjugate ionospheres and the tilt of the Earth's magnetic field. J. Geophys. Res. **91**(A8), 9017–9021 (1986)

A.J. Ridley, M.W. Liemohn, A model-derived storm time asymmetric ring current driven electric field description. J. Geophys. Res. **107**(A8), 1151 (2002)

A.J. Ridley, T.I. Gombosi, D.L. DeZeeuw, Ionospheric control of the magnetosphere: conductance. Ann. Geophys. **22**(2), 567–584 (2004)

B.R. Sandel, M.H. Denton, Global view of refilling of the plasmasphere. Geophys. Res. Lett. **34**, L17102 (2007)

B.R. Sandel, A.L. Broadfoot, C.C. Curtis, R.A. King, T.C. Stone, R.H. Hill, J. Chen, O.H.W. Siegmund, R. Raffanti, D.D. Allred, R.S. Turley, D.L. Gallagher, The extreme ultraviolet imager investigation for the IMAGE mission. Space Sci. Rev. **91**(1–2), 197–242 (2000)

S. Sazykin, R.W. Spiro, R.A. Wolf, F.R. Toffoletto, N. Tsyganenko, J. Goldstein, M.R. Hairston, Modeling inner magnetospheric electric fields: Latest self-consistent results, in *The Inner Magnetosphere: Physics and Modeling*, ed. by T.I. Pulkkinen, N.A. Tsyganenko, R.H.W. Friedel. Geophysical Monograph Series, vol. 155 (American Geophysical Union, Washington, 2005), pp. 263–269

S. Schäfer, K.H. Glassmeier, P.T.I. Eriksson, V. Pierrard, K.H. Fornaçon, L.G. Blomberg, Spatial and temporal characteristics of poloidal waves in the terrestrial plasmasphere: a CLUSTER case study. Ann. Geophys. **25**(4), 1011–1024 (2007)

S. Schäfer, K.H. Glassmeier, P.T.I. Eriksson, P.N. Mager, V. Pierrard, K.H. Fornaçon, L.G. Blomberg, Spatiotemporal structure of a poloidal Alfvén wave detected by Cluster adjacent to the dayside plasmapause. Ann. Geophys. **26**(7), 1805–1817 (2008)

R.W. Schunk, A mathematical model of the middle and high latitude ionosphere. Pure Appl. Geophys. **127**(2–3), 255–303 (1988)

R.W. Schunk, D.S. Watkins, Comparison of solutions to the thirteen-moment and standard transport equations for low speed thermal proton flows. Planet. Space Sci. **27**(4), 433–444 (1979)

R.W. Schunk, D.S. Watkins, Electron temperature anisotropy in the polar wind. J. Geophys. Res. **86**(A1), 91–102 (1981)

R.W. Schunk, L. Scherliess, J.S. Sojka, D.C. Thompson, D.N. Anderson, M. Codrescu, C. Minter, T.J. Fuller-Rowell, R.A. Heelis, M. Hairston, B.M. Howe, Global Assimilation of Ionospheric Measurements (GAIM). Radio Sci. **39**(1), RS1S02 (2004)

N. Singh, Refilling of a plasmaspheric flux tube: Microscopic plasma processes, in *Modeling Magnetospheric Plasma*, ed. by T.E. Moore, J.H. Waite. Geophysical Monograph Series, vol. 44 (American Geophysical Union, Washington, 1988), pp. 87–99

N. Singh, J.L. Horwitz, Plasmaspheric refilling: Recent observations and modelling. J. Geophys. Res. **97**(A2), 1049–1079 (1992)

N. Singh, R.W. Schunk, H. Thiemann, Temporal features of the refilling of a plasmaspheric flux tube. J. Geophys. Res. **91**(A12), 13433–13454 (1986)

M. Smiddy, M.C. Kelley, W. Burke, F. Rich, R. Sagalyn, B. Shuman, R. Hays, S. Lai, Intense poleward-directed electric fields near the ionospheric projection of the plasmapause. Geophys. Res. Lett. **4**(11), 543–546 (1977)

D.J. Southwood, M.G. Kivelson, Magnetospheric interchange instability. J. Geophys. Res. **92**(A1), 109–116 (1987)

M. Spasojević, J. Goldstein, D.L. Carpenter, U.S. Inan, B.R. Sandel, M.B. Moldwin, B.W. Reinisch, Global response of the plasmasphere to a geomagnetic disturbance. J. Geophys. Res. **108**(A9), 1340 (2003)

M. Spasojević, H.U. Frey, M.F. Thomsen, S.A. Fuselier, S.P. Gary, B.R. Sandel, U.S. Inan, The link between a detached subauroral proton arc and a plasmaspheric plume. Geophys. Res. Lett. **31**, L04803 (2004)

R.W. Spiro, M. Harel, R.A. Wolf, P.H. Reiff, Quantitative simulation of a magnetospheric substorm 3. Plasmaspheric electric fields and evolution of the plasmapause. J. Geophys. Res. **86**(A4), 2261–2272 (1981)

D.P. Stern, The motion of a proton in the equatorial magnetosphere. J. Geophys. Res. **80**(4), 595–599 (1975)

D.F. Strobel, T.R. Young, R.R. Meier, T.P. Coffey, A.W. Ali, The nighttime ionosphere: E region and lower F region. J. Geophys. Res. **79**(22), 3171–3178 (1974)

S.W.Y. Tam, F. Yasseen, T. Chang, S.B. Ganguli, Self-consistent kinetic photoelectron effect on the polar wind. Geophys. Res. Lett. **22**(16), 2107–2110 (1995)

S.W.Y. Tam, T. Chang, V. Pierrard, Kinetic modeling of the polar wind. J. Atmos. Sol.-Terr. Phys. **69**(16), 1984–2027 (2007)
H.A. Taylor Jr., W.J. Walsh, The light-ion trough, the main trough, and the plasmapause. J. Geophys. Res. **77**(34), 6716–6723 (1972)
N.A. Tsyganenko, D.P. Stern, Modeling the global magnetic field of the large-scale Birkeland current systems. J. Geophys. Res. **101**(A12), 27187–27198 (1996)
J.N. Tu, J.L. Horwitz, P. Song, X.Q. Huang, B.W. Reinisch, P.G. Richards, Simulating plasmaspheric field-aligned density profiles measured with IMAGE/RPI: Effects of plasmasphere refilling and ion heating. J. Geophys. Res. **108**(A1), 1017 (2003)
J.N. Tu, J.L. Horwitz, P.A. Nsumei, P. Song, X.Q. Huang, B.W. Reinisch, Simulation of polar cap field-aligned electron density profiles measured with the IMAGE radio plasma imager. J. Geophys. Res. **109**, A07206 (2004)
J. Tu, P. Song, B.W. Reinisch, J.L. Green, Smooth electron density transition from plasmasphere to the sub-auroral region. J. Geophys. Res. **112**, A05227 (2007)
H. Volland, A semiempirical model of large-scale magnetospheric electric fields. J. Geophys. Res. **78**(1), 171–180 (1973)
P.A. Webb, E.A. Essex, A dynamic global model of the plasmasphere. J. Atmos. Sol.-Terr. Phys. **66**(12), 1057–1073 (2004)
D.R. Weimer, A flexible, IMF dependent model of high-latitude electric potentials having "space weather" applications. Geophys. Res. Lett. **23**(18), 2549–2552 (1996)
D.R. Weimer, Substorm influence on the ionosphere electric potentials and currents. J. Geophys. Res. **104**(A1), 185–197 (1999)
D.R. Weimer, An improved model of ionospheric electric potentials including substorm perturbations and application to the geospace environment modeling November 24, 1996, event. J. Geophys. Res. **106**(A1), 407–416 (2001)
L.A. Weiss, R.L. Lambour, R.C. Elphic, M.F. Thomsen, Study of plasmaspheric evolution using geosynchronous observations and global modeling. Geophys. Res. Lett. **24**(5), 599–602 (1997)
G.R. Wilson, J.L. Horwitz, J. Lin, A semikinetic model for early stage plasmasphere refilling 1. Effects of Coulomb collisions. J. Geophys. Res. **97**(A2), 1109–1119 (1992)
G.R. Wilson, J.L. Horwitz, J. Lin, Semikinetic modeling of plasma flow on outer plasmaspheric field lines. Adv. Space Res. **13**(4), 107–116 (1993)
F. Yasseen, J.M. Retterer, T. Chang, J.D. Winningham, Monte-Carlo modeling of polar wind photoelectron distributions with anomalous heat flux. Geophys. Res. Lett. **16**(9), 1023–1026 (1989)
I. Yoshikawa, A. Yamazaki, K. Yamashita, Y. Takizawa, M. Nakamura, Which is a significant contributor for outside of the plasmapause, an ionospheric filling or leakage of plasmaspheric materials?: Comparison of He II (304 Å) images. J. Geophys. Res. **108**(A2), 1080 (2003)
D.T. Young, J. Geiss, H. Balsiger, P. Eberhardt, A. Ghielmetti, H. Rosenbauer, Discovery of $He^{2+}$ and $O^{2+}$ ions of terrestrial origin in the outer magnetosphere. Geophys. Res. Lett. **4**(12), 561–564 (1977)